



Research article

A novel approach to modelling the spatial spread of airborne diseases: an epidemic model with indirect transmission

Jummy F. David^{1 2 *}, **Sarafa A. Iyaniwura**^{1*}, **Michael J. Ward**¹ and **Fred Brauer**¹

¹ Department of Mathematics, University of British Columbia, Vancouver, B.C., Canada.

² Interdisciplinary Studies, University of British Columbia, Vancouver, B.C., Canada.

* **Correspondence:** Email: jummy30@math.ubc.ca & iyaniwura@math.ubc.ca

Abstract: We formulated and analyzed a class of coupled partial and ordinary differential equation (PDE-ODE) model to study the spread of airborne diseases. Our model describes human populations with patches and the movement of pathogens in the air with linear diffusion. The diffusing pathogens are coupled to the SIR dynamics of each population patch using an integro-differential equation. Susceptible individuals become infected at some rate whenever they are in contact with pathogens (indirect transmission), and the spread of infection in each patch depends on the density of pathogens around the patch. In the limit where the pathogens are diffusing fast, a matched asymptotic analysis is used to reduce the coupled PDE-ODE model into a nonlinear system of ODEs, which is then used to compute the basic reproduction number and final size relation for different scenarios. Numerical simulations of the reduced system of ODEs and the full PDE-ODE model are consistent, and they predict a decrease in the spread of infection as the diffusion rate of pathogens increases. Furthermore, we studied the effect of patch location on the spread of infections for the case of two population patches. Our model predicts higher infections when the patches are closer to each other.

Keywords: disease dynamics, epidemics, airborne disease, indirect transmission, matched asymptotic analysis, Green's function, ODE, PDE.

1. Introduction

Airborne diseases are well studied in epidemiology and public health, and still remain a serious public health concern today. Many airborne diseases are transmitted directly (host-host) and/or indirectly (host-source-host) through actions such as coughing, sneezing and sometimes vomiting [24]. For example, viral diseases (measles, influenza) and bacterial infections (tuberculosis) are transmitted via an airborne route. In addition, there has been evidence that airborne transmission plays a significant role in the spread of many opportunistic pathogens causing several acquired nosocomial (hospital) infections

[2]. Some mathematical models have been used to study the transmission of airborne diseases using direct and indirect transmission pathways. Noakes et al. in [24] studied the transmission of airborne infections in enclosed spaces using an *SEIR* model to show how changes to both physical environment and infection control could be a potential limitation in the spread of airborne infections. Issarow et al. in [18] developed a model to predict the risk of airborne infectious diseases such as tuberculosis in confined spaces using exhaled air. Several approaches including but not limited to the framework in [29] have been used to study the dynamics of an *SIS* model with diffusion, [15] to assess the impact of heterogeneity of environment and advection on the persistence and infectious diseases eradication, and [21] to evaluate population migration using an *SIS* epidemic model with diffusion. In addition, several PDE models such as [29, 31] were also used to study the effect of diffusion. However, despite all these models and previous studies, it has largely been an open problem to evaluate the effect of diffusion on the spread of infections between one or two populations. To our knowledge none of these works has assessed the impact of diffusion using a coupled PDE-ODE SIR model with an indirect transmission pathway.

In this paper, we consider an airborne disease as any disease caused by pathogen and transmitted through the air. Such diseases include, but are not limited to, cholera, chickenpox, influenza, measles, smallpox, and tuberculosis, among others. We focus on an indirect transmission pathways and derive fundamental quantities such as the basic reproduction number (\mathcal{R}_0) and the final size relation. To incorporate the limitation of the impact of diffusion among homogeneous and heterogeneous mixing population, we propose a coupled PDE-ODE model similar to the one used in [16] to model communication between dynamically active signaling compartments. Our model extends the models presented in [7] and [13] by incorporating diffusion of pathogens. This allows us to theoretically and numerically analyze how diffusion affects the spread of air-transmitted diseases, in which the human populations are confined to distinct spatially segregated regions. The novelty of our approach is that through a PDE-ODE system we model the spread of airborne diseases allowing for person-air-person transmission. Overall, our modeling framework provides an alternative way to describe the epidemics of airborne diseases.

The outline of this paper is as follows. In Section 2, a new coupled PDE-ODE model of epidemics is formulated, and this model is non-dimensionalized in Section 2.1. In Section 2.2, matched asymptotic expansion methods is used to reduce the dimensionless coupled PDE-ODE model into a nonlinear system of ODEs in the limit where the pathogens are diffusing very fast. In Section 3, we study the dimensionless coupled PDE-ODE model for a single population patch numerically and compare the result to that of the reduced system of ODEs. We also use the reduced system of ODEs to compute the basic reproduction number and final size relation. A similar study is performed for the case of two population patches in Section 4. In Section 5, we study the effect of patch location on the spread of infection for two population patches. The paper concludes with a brief discussion in Section 6.

2. Model formulation

In this section, we formulate and analyze a coupled PDE-ODE model for studying the spread of airborne diseases. This model is non-dimensionalized and later reduced into a nonlinear ODE system in the limit where the diffusivity of pathogens is large.

We begin by representing human populations by localized patches with partially transmitting bound-

aries through which pathogens are shed into the atmosphere by infected individuals. These pathogens are assumed to diffuse and decay at a constant rate in the air (bulk region), while the spread of infection in each patch depends on the density of pathogens around the patch. Pathogens are not explicitly modeled in the patches; likewise the movement of individuals between patches is not accounted for. A susceptible individual becomes infected by coming in contact with pathogens (*indirect transmission pathway*). Let $\Omega \subset \mathbb{R}^2$ be our 2-D bounded domain of interest containing m population patches represented by Ω_j for $j = 1, \dots, m$, and separated by an $O(1)$ distance from each other and from the boundary of the domain $\partial\Omega$. In the region $\Omega \setminus \cup_{j=1}^m \Omega_j$ (bulk region) between the patches, the spatio-temporal density of pathogens $\mathcal{P}(\mathbf{X}, T)$ satisfies the partial differential equation (PDE) given by

$$\frac{\partial \mathcal{P}}{\partial T} = D_B \Delta \mathcal{P} - \delta \mathcal{P}, \quad T > 0, \quad \mathbf{X} \in \Omega \setminus \cup_{j=1}^m \Omega_j; \quad (2.1a)$$

$$\partial_{n_{\mathbf{X}}} \mathcal{P} = 0, \quad \mathbf{X} \in \partial\Omega; \quad D_B \partial_{n_{\mathbf{X}}} \mathcal{P} = -r_j \mathcal{I}_j, \quad \mathbf{X} \in \partial\Omega_j, \quad j = 1, \dots, m, \quad (2.1b)$$

where $D_B > 0$ denotes the diffusion rate of pathogens in the bulk region, δ is the dimensional decay rate of pathogens, $r_j > 0$ is the dimensional shedding rate of pathogen by an infected individual in the j^{th} patch, and $\partial_{n_{\mathbf{X}}}$ is the outward normal derivative on the boundary of the domain Ω . The dynamics of the diffusing pathogens is coupled to the population dynamics of the j^{th} patch using the integro-differential system of equations given by

$$\frac{d\mathcal{S}_j}{dT} = -\mu_j \mathcal{S}_j \int_{\partial\Omega_j} (\mathcal{P}/p_c) dS_{\mathbf{X}}; \quad (2.1c)$$

$$\frac{d\mathcal{I}_j}{dT} = \mu_j \mathcal{S}_j \int_{\partial\Omega_j} (\mathcal{P}/p_c) dS_{\mathbf{X}} - \alpha_j \mathcal{I}_j; \quad (2.1d)$$

$$\frac{d\mathcal{R}_j}{dT} = \alpha_j \mathcal{I}_j, \quad j = 1, \dots, m, \quad (2.1e)$$

where \mathcal{S}_j , \mathcal{I}_j , and \mathcal{R}_j denote the population of susceptible, infected, and removed individuals in the j^{th} patch, respectively, with $\mathcal{N}_j(T) = \mathcal{S}_j(T) + \mathcal{I}_j(T) + \mathcal{R}_j(T)$. The parameters μ_j and α_j are the dimensional transmission and recovery rates, respectively, for individuals in the j^{th} patch, and p_c is a typical value for the density of pathogens. The integrals in (2.1c) and (2.1d) are over the boundary of the j^{th} patch, and are used to account for all the pathogens around the patch. These terms show that the spread of infection within a patch depends on the density of pathogens around it. It is important to emphasize that our model does not account for pathogens in the patches. The Robin boundary condition $D_B \partial_{n_{\mathbf{X}}} \mathcal{P} = -r_j \mathcal{I}_j$ on the boundary of the j^{th} patch accounts for the amount of pathogen shed into the atmosphere by infected individuals in the patch. This condition shows that the amount of pathogens shed into the atmosphere from the j^{th} patch depends on the population of infected individuals within the patch.

2.1. Non-dimensionalization of the coupled PDE-ODE model

In this subsection, we non-dimensionalize the coupled PDE-ODE model (2.1). The dimensions of the variables and parameters of the model are given as follow:

$$\begin{aligned} [\mathcal{P}] &= \frac{\text{pathogens}}{(\text{length})^2}, & [D_B] &= \frac{(\text{length})^2}{\text{time}}, & [p_c] &= \text{pathogens}, & [T] &= \text{time}, & [\mathbf{X}] &= \text{length}, \\ [\delta] &= [\alpha_j] = \frac{1}{\text{time}}, & [\mathcal{N}_j] &= [\mathcal{S}_j] = [\mathcal{I}_j] = [\mathcal{R}_j] = \text{individuals}, & [\mu_j] &= \frac{\text{length}}{\text{time}}, \\ [r_j] &= \frac{\text{pathogens}}{\text{individual} \times \text{time} \times \text{length}}, & & & & & & & & j = 1, \dots, m, \end{aligned} \quad (2.2)$$

where $[\gamma]$ represents the dimension of γ . Assuming that the patches are circular with common radius R , which is small relative to the length-scale L of the 2-D domain Ω , we introduce a small scaling parameter $\varepsilon = R/L \ll 1$ and the following dimensionless variables

$$P = \frac{L^2}{p_c} \mathcal{P}, \quad S_j = \frac{\mathcal{S}_j}{\mathcal{N}_j}, \quad I_j = \frac{\mathcal{I}_j}{\mathcal{N}_j}, \quad R_j = \frac{\mathcal{R}_j}{\mathcal{N}_j}, \quad \mathbf{x} = \frac{\mathbf{X}}{L}, \quad t = \delta T. \quad (2.3)$$

In this way, S_j, I_j , and R_j are the proportion of susceptible, infected, and removed individuals in the j^{th} patch, respectively, and $P \equiv P(\mathbf{x}, t)$ is the dimensionless density of the pathogens at position \mathbf{x} at time t . Upon substituting (2.3) into (2.1), we derive that the dimensionless spatio-temporal density of pathogens $P(\mathbf{x}, t)$ satisfies

$$\frac{\partial P}{\partial t} = D \Delta P - P, \quad t > 0, \quad \mathbf{x} \in \Omega \setminus \cup_{j=1}^m \Omega_j; \quad (2.4a)$$

$$\partial_{n_x} P = 0, \quad \mathbf{x} \in \partial\Omega; \quad D \partial_{n_x} P = -r_j \left(\frac{\mathcal{N}_j L}{\delta p_c} \right) I_j, \quad \mathbf{x} \in \partial\Omega_j, \quad j = 1, \dots, m, \quad (2.4b)$$

where $D \equiv D_B/(\delta L^2)$ is the effective diffusion rate of the pathogens. From the system of ODEs ((2.1c) - (2.1e)) for the population dynamics of the j^{th} patch, we derive the dimensionless system

$$\begin{aligned} \frac{dS_j}{dt} &= - \left(\frac{\mu_j}{\delta L} \right) S_j \int_{\partial\Omega_{\varepsilon j}} P \, ds_{\mathbf{x}}; \\ \frac{dI_j}{dt} &= \left(\frac{\mu_j}{\delta L} \right) S_j \int_{\partial\Omega_{\varepsilon j}} P \, ds_{\mathbf{x}} - \phi_j I_j; \\ \frac{dR_j}{dt} &= \phi_j I_j, \quad j = 1, \dots, m, \end{aligned} \quad (2.5)$$

where $\Omega_{\varepsilon j} = \{\mathbf{x} : |\mathbf{x}_j - \mathbf{x}| < \varepsilon\}$ represents the j^{th} patch of radius $\varepsilon \ll 1$ with center at \mathbf{x}_j and boundary $\partial\Omega_{\varepsilon j}$. It is important to remark that we have used the scaling $dS_{\mathbf{x}} = L ds_{\mathbf{x}}$ in the integrals on the boundary of the patches. Since the patches are relatively small compared to the length-scale of the domain, we assume that $(\mu_j/\delta L)$ and $r_j(\mathcal{N}_j L/\delta p_c)$ are $O(1/\varepsilon)$ in order to effectively capture the density of the pathogen shed into the atmosphere. Hence, we set

$$\frac{\beta_j}{2\pi\varepsilon} = \frac{\mu_j}{\delta L} \quad \text{and} \quad \frac{\sigma_j}{2\pi\varepsilon} = r_j \frac{\mathcal{N}_j L}{\delta p_c}, \quad (2.6)$$

such that β_j and σ_j are $O(1)$. This rescaling enables us to write the dimensionless transmission and shedding rates, β_j and σ_j , respectively, as functions of the circumference of the j^{th} patch. Substituting (2.6) into (2.4) and (2.5), we have that the dimensionless density of the pathogens $P(\mathbf{x}, t)$ satisfies

$$\frac{\partial P}{\partial t} = D \Delta P - P, \quad t > 0, \quad \mathbf{x} \in \Omega \setminus \cup_{j=1}^m \Omega_{\varepsilon j}; \quad (2.7a)$$

$$\partial_{n_x} P = 0, \quad \mathbf{x} \in \partial\Omega; \quad 2\pi\varepsilon D \partial_{n_x} P = -\sigma_j I_j, \quad \mathbf{x} \in \partial\Omega_{\varepsilon j}, \quad j = 1, \dots, m, \quad (2.7b)$$

which is coupled to the dimensionless SIR dynamics of the j^{th} patch through the integro-differential equations given by

$$\begin{aligned} \frac{dS_j}{dt} &= -\frac{\beta_j S_j}{2\pi\varepsilon} \int_{\partial\Omega_{\varepsilon j}} P \, ds_x; \\ \frac{dI_j}{dt} &= \frac{\beta_j S_j}{2\pi\varepsilon} \int_{\partial\Omega_{\varepsilon j}} P \, ds_x - \phi_j I_j; \\ \frac{dR_j}{dt} &= \phi_j I_j, \quad j = 1, \dots, m, \end{aligned} \quad (2.7c)$$

where β_j , σ_j and ϕ_j are the dimensionless transmission, shedding and recovery rates for the j^{th} patch, respectively, and are given by

$$\beta_j = \frac{2\pi\varepsilon}{\delta L} \mu_j, \quad \sigma_j = \frac{2\pi\varepsilon}{\delta} r_j N_j L \quad \text{and} \quad \phi_j = \frac{\alpha_j}{\delta}. \quad (2.8)$$

In the next subsection, we study the dimensionless coupled PDE-ODE model (2.7) in the limit $D = O(\nu^{-1})$, where $\nu = -1/\log \varepsilon$ and $\varepsilon \ll 1$ using the method of matched asymptotic expansions, tailored to problems involving strong localized spatial perturbations [28], [16].

2.2. Asymptotic analysis of the dimensionless coupled PDE-ODE model

Here, the dimensionless coupled PDE-ODE model (2.7) is analyzed in the limit $D = O(\nu^{-1})$, where $\nu \equiv -1/\log \varepsilon$ for $\varepsilon \ll 1$, using the method of matched asymptotic expansions. This analysis is used to reduce the coupled model into a nonlinear system of ODEs, which is then used to determine the basic reproduction number and final size relation of epidemics.

We begin our analysis by rescaling the diffusion rate of pathogens as

$$D = \frac{D_0}{\nu}, \quad \text{where} \quad D_0 = O(1) \quad \text{and} \quad \nu = -\frac{1}{\log \varepsilon} \ll 1. \quad (2.9)$$

Substituting $D = D_0/\nu$ into (2.7a) and (2.7b), we obtain

$$\frac{\partial P}{\partial t} = \frac{D_0}{\nu} \Delta P - P, \quad t > 0, \quad \mathbf{x} \in \Omega \setminus \cup_{j=1}^m \Omega_{\varepsilon j}; \quad (2.10a)$$

$$\partial_{n_x} P = 0, \quad \mathbf{x} \in \partial\Omega; \quad 2\pi\varepsilon \frac{D_0}{\nu} \partial_{n_x} P = -\sigma_j I_j, \quad \mathbf{x} \in \partial\Omega_{\varepsilon j}, \quad j = 1, \dots, m. \quad (2.10b)$$

Since the pathogens shed by infected individuals go into the air through the boundary of the patches, one would expect the density of pathogens around each patch to be high relative to the regions far

away from the patches. As a result of this, we construct an inner region at an $\mathcal{O}(\varepsilon)$ neighborhood of each patch, and introduce the local variables $\mathbf{y} = \varepsilon^{-1}(\mathbf{x} - \mathbf{x}_j)$ and $P(\mathbf{x}) = Q_j(\varepsilon\mathbf{y} + \mathbf{x}_j)$, with $|\mathbf{y}| = \rho$ for $j = 1, \dots, m$. Upon writing (2.10a) and (2.10b) in terms of the inner variables, we obtain for $\varepsilon \ll 1$ the limiting inner problem

$$\begin{aligned} \Delta_\rho Q_j &= 0, \quad t > 0, \quad \rho > 1; \\ 2\pi \frac{D_0}{\nu} \partial_\rho Q_j &= -\sigma_j I_j, \quad \rho = 1, \quad j = 1, \dots, m, \end{aligned} \quad (2.11)$$

where $\Delta_\rho \equiv \partial_{\rho\rho} + \rho^{-1}\partial_\rho$ is the radially symmetric part of the Laplacian in 2-D. In this inner region, we expand $Q_j(\rho, t)$ as

$$Q_j = Q_{0j} + \frac{\nu}{D_0} Q_{1j} + \dots \quad (2.12)$$

Upon substituting this expansion into (2.11), and collecting terms in powers of ν , we obtain the leading-order inner problem

$$\Delta_\rho Q_{0j} = 0, \quad t > 0, \quad \rho > 1; \quad \partial_\rho Q_{0j} = 0 \quad \text{on} \quad \rho = 1, \quad j = 1, \dots, m. \quad (2.13)$$

Observe that any constant or function of time is a solution to this problem, so that $Q_{0j} \equiv Q_{0j}(t)$. The next-order inner problem is given by

$$\Delta_\rho Q_{1j} = 0, \quad t > 0, \quad \rho > 1; \quad 2\pi \partial_\rho Q_{1j} = -\sigma_j I_j \quad \text{on} \quad \rho = 1, \quad j = 1, \dots, m, \quad (2.14)$$

and its solution is readily calculated as

$$Q_{1j} = \left(\frac{-\sigma_j I_j}{2\pi} \right) \log \rho + c_j, \quad j = 1, \dots, m, \quad (2.15)$$

where c_j , for $j = 1, \dots, m$, are constants to be determined. Substituting the solutions Q_{0j} and Q_{1j} into the inner expansion (2.12), and writing the resulting expression in terms of the outer variables, we obtain a two term asymptotic expansion of the inner solution

$$Q_j = \left(Q_{0j}(t) - \frac{\sigma_j I_j}{2\pi D_0} \right) + \frac{\nu}{D_0} \left(-\frac{\sigma_j I_j}{2\pi} \log |\mathbf{x} - \mathbf{x}_j| + c_j \right) + \dots \quad (2.16)$$

Next, from (2.4a) and (2.4b), we construct the outer problem for the density of pathogens, which is valid far away from the patches, as

$$\frac{\partial P}{\partial t} = D \Delta P - P, \quad t > 0, \quad \mathbf{x} \in \Omega \setminus \{\mathbf{x}_1, \dots, \mathbf{x}_m\}; \quad \partial_n P = 0, \quad \mathbf{x} \in \partial\Omega, \quad (2.17)$$

where $\mathbf{x}_1, \dots, \mathbf{x}_m$ are the centers of the patches. In this region, we expand the outer solution as

$$P = P_0 + \frac{\nu}{D_0} P_1 + \dots \quad (2.18)$$

Substituting (2.18) into (2.17), and collecting terms in powers of ν , we obtain the leading-order outer problem given by

$$\Delta P_0 = 0, \quad t > 0, \quad \mathbf{x} \in \Omega \setminus \{\mathbf{x}_1, \dots, \mathbf{x}_m\}; \quad \partial_n P_0 = 0, \quad \mathbf{x} \in \partial\Omega. \quad (2.19)$$

Observe that this problem is similar to the leading-order inner problem (2.13) and any constant or function of time satisfies it. As a result of this, we chose the leading-order outer solution to be $P_0 \equiv P_0(t)$. The next order outer problem for P_1 is given by

$$\Delta P_1 = P_0 + P_{0\nu}, \quad \mathbf{x} \in \Omega \setminus \{\mathbf{x}_1, \mathbf{x}_2, \dots, \mathbf{x}_m\}; \quad \partial_n P_1 = 0, \quad \mathbf{x} \in \partial\Omega. \quad (2.20)$$

Upon matching the inner solution (2.16) and the outer expansion (2.18), we obtain the following required singularity behavior for the outer solution as $\mathbf{x} \rightarrow \mathbf{x}_j$:

$$P_0(t) + \frac{\nu}{D_0} P_1 + \dots \sim \left(Q_{0j}(t) - \frac{\sigma_j I_j}{2\pi D_0} \right) + \frac{\nu}{D_0} \left(-\frac{\sigma_j I_j}{2\pi} \log |\mathbf{x} - \mathbf{x}_j| + c_j \right) + \dots, \quad \mathbf{x} \rightarrow \mathbf{x}_j. \quad (2.21)$$

In this way, we obtain the matching conditions

$$P_0(t) \sim Q_{0j}(t) - \frac{\sigma_j I_j}{2\pi D_0} \quad \text{and} \quad P_1 \sim -\left(\frac{\sigma_j I_j}{2\pi} \right) \log |\mathbf{x} - \mathbf{x}_j| \quad \text{as} \quad \mathbf{x} \rightarrow \mathbf{x}_j. \quad (2.22)$$

The first condition yields that $Q_{0j}(t) = P_0(t) + \sigma_j I_j / (2\pi D_0)$ for each $j = 1, \dots, m$. The ODE for $P_0(t)$ is derived from a solvability condition on the problem for P_1 . To do so, it is convenient to write the singularity behaviour of P_1 given in (2.22) as a delta function forcing for the PDE in (2.20). In this way, the outer problem for P_1 is equivalent to

$$\Delta P_1 = P_0 + P'_0 + \sum_{i=1}^m (-\sigma_i I_i) \delta(\mathbf{x} - \mathbf{x}_i), \quad \mathbf{x} \in \Omega; \quad \partial_n P_1 = 0, \quad \mathbf{x} \in \partial\Omega. \quad (2.23)$$

Integrating (2.23) over the domain Ω and using the divergence theorem, we obtain an ODE for the leading-order density of pathogens $P_0(t)$ in the bulk region given by

$$P'_0 = -P_0 + \frac{1}{|\Omega|} \sum_{i=1}^m \sigma_i I_i. \quad (2.24)$$

This ODE is the solvability condition for the $O(\nu)$ outer problem (2.23).

To solve the outer problem (2.23), we introduce the unique Neumann Green's function $G(\mathbf{x}; \mathbf{x}_j)$, which satisfies

$$\Delta G = \frac{1}{|\Omega|} - \delta(\mathbf{x} - \mathbf{x}_j), \quad \mathbf{x} \in \Omega; \quad \partial_n G = 0, \quad \mathbf{x} \in \partial\Omega; \quad (2.25a)$$

$$G(\mathbf{x}; \mathbf{x}_j) \sim -\frac{1}{2\pi} \log |\mathbf{x} - \mathbf{x}_j| + \mathfrak{R}_j, \quad \text{as} \quad \mathbf{x} \rightarrow \mathbf{x}_j, \quad \text{and} \quad \int_{\Omega} G \, d\mathbf{x} = 0, \quad (2.25b)$$

where $\mathfrak{R}_j \equiv \mathfrak{R}(\mathbf{x}_j)$ is the regular part of $G(\mathbf{x}; \mathbf{x}_j)$ at $\mathbf{x} = \mathbf{x}_j$. Without loss of generality, we impose $\int_{\Omega} P_1 \, d\mathbf{x} = 0$, so that the spatial average of P in the bulk region is P_0 . Therefore, the solution to the outer problem (2.23) is written in terms of the Neumann Green's function $G(\mathbf{x}; \mathbf{x}_j)$ as

$$P_1 = \sum_{i=1}^m \sigma_i I_i G(\mathbf{x}; \mathbf{x}_i). \quad (2.26)$$

Upon substituting (2.26) into the outer expansion (2.18), we obtain a two-term asymptotic expansion of the outer solution in the bulk region as

$$P = P_0 + \frac{\nu}{D_0} \sum_{i=1}^m \sigma_i I_i G(\mathbf{x}; \mathbf{x}_i) + \dots \quad (2.27)$$

Now, we expand (2.26) as $\mathbf{x} \rightarrow \mathbf{x}_j$, and substitute the singularity behaviour of the Neumann Green's function $G(\mathbf{x}, \mathbf{x}_j)$ given in (2.25b) into the corresponding expansion to get

$$P_1 \sim \sigma_j I_j \left(-\frac{1}{2\pi} \log |\mathbf{x} - \mathbf{x}_j| + \mathfrak{R}_j \right) + \sum_{i \neq j}^m \sigma_i I_i G(\mathbf{x}_j; \mathbf{x}_i) \quad \text{as } \mathbf{x} \rightarrow \mathbf{x}_j, \quad j = 1, \dots, m. \quad (2.28)$$

Matching the inner and outer solutions, we derive the constants c_j in terms of the Neumann Green's function as

$$c_j = \sigma_j I_j \mathfrak{R}_j + \sum_{i \neq j}^m \sigma_i I_i G(\mathbf{x}_j; \mathbf{x}_i), \quad j = 1, \dots, m. \quad (2.29)$$

Thus, substituting (2.29) into (2.16), we derive a two-term asymptotic expansion of the inner solution $Q_j(\rho, t)$, valid in an $O(\varepsilon)$ neighborhood of the j^{th} patch, given by

$$Q_j = \left(P_0(t) + \frac{\sigma_j I_j}{2\pi D_0} \right) + \frac{\nu}{D_0} \left[-\left(\frac{\sigma_j I_j}{2\pi} \right) \log \rho + \sigma_j I_j \mathfrak{R}_j + \sum_{i \neq j}^m \sigma_i I_i G(\mathbf{x}_j; \mathbf{x}_i) \right] + \dots, \quad j = 1, \dots, m. \quad (2.30)$$

Lastly, by substituting the inner solution (2.30) into the SIR system in (2.7c), and evaluating the integrals over the boundary of the j^{th} patch, we obtain a nonlinear system of ODEs for the leading-order density of pathogens in the bulk region coupled to the population dynamics of the j^{th} patch. This system is given by

$$\frac{dP_0}{dt} = -P_0 + \frac{1}{|\Omega|} \sum_{j=1}^m \sigma_j I_j, \quad (2.31a)$$

which is coupled to

$$\begin{aligned} \frac{dS_j}{dt} &= -\beta_j S_j \left(P_0(t) + \frac{\sigma_j I_j}{2\pi D_0} \right) - \frac{\nu}{D_0} \beta_j S_j \Psi_j, \\ \frac{dI_j}{dt} &= \beta_j S_j \left(P_0(t) + \frac{\sigma_j I_j}{2\pi D_0} \right) + \frac{\nu}{D_0} \beta_j S_j \Psi_j - \phi_j I_j, \\ \frac{dR_j}{dt} &= \phi_j I_j, \quad j = 1, \dots, m. \end{aligned} \quad (2.31b)$$

Here, $\Psi_j = (\mathcal{G}\Phi)_j$ is the j^{th} entry of the vector $\mathcal{G}\Phi$, with $\Phi = (\sigma_1 I_1, \dots, \sigma_m I_m)^T$ and \mathcal{G} is the Neumann Green's matrix whose entries are defined by

$$(\mathcal{G})_{jj} = \mathfrak{R}_j \equiv \mathfrak{R}(\mathbf{x}_j) \quad \text{for } i = j \quad \text{and} \quad (\mathcal{G})_{ij} = G(\mathbf{x}_i; \mathbf{x}_j) \quad \text{for } i \neq j \quad \text{with} \quad (\mathcal{G})_{ij} = (\mathcal{G})_{ji}. \quad (2.32)$$

The function $G(\mathbf{x}_j; \mathbf{x}_i)$ is the Neumann Green's function satisfying (2.25) and $\mathfrak{R}_j \equiv \mathfrak{R}(\mathbf{x}_j)$ is its regular part at the point $\mathbf{x} = \mathbf{x}_j$. In our analysis, $D_0 = O(1)$ and $\nu = -1/\log \varepsilon \ll 1$. Therefore, as ε tends to zero, ν also approaches zero, and so to leading-order we can neglect the $O(\nu)$ terms in (2.31b). Replacing the leading-order density of pathogens P_0 with p in (2.31), we derive the leading-order system of ODEs given by

$$\frac{dp}{dt} = -p + \frac{1}{|\Omega|} \sum_{j=1}^m \sigma_j I_j, \quad (2.33a)$$

$$\frac{dS_j}{dt} = -\beta_j S_j \left(p(t) + \frac{\sigma_j I_j}{2\pi D_0} \right), \quad j = 1, \dots, m, \quad (2.33b)$$

$$\frac{dI_j}{dt} = \beta_j S_j \left(p(t) + \frac{\sigma_j I_j}{2\pi D_0} \right) - \phi_j I_j, \quad j = 1, \dots, m, \quad (2.33c)$$

$$\frac{dR_j}{dt} = \phi_j I_j, \quad j = 1, \dots, m, \quad (2.33d)$$

Observe that we started with the dimensionless coupled PDE-ODE model (2.7) for studying the spread of airborne disease with indirect transmission, and arrived at the leading-order reduced system of ODEs (2.33) in the limit $D = O(\nu^{-1})$. This system of ODEs also models indirect transmission of infections, even though, the terms with $\sigma_j I_j/(2\pi D_0)$ in (2.33b) and (2.33c) make it look like infection is transmitted from person-to-person through direct interaction. This term does not model direct transmission; rather, it accounts for the pathogens shed by infected individuals in a patch. The density of these pathogens depend on the scaled-diffusion rate $D_0 > 0$. When the pathogens diffuse more slowly (smaller values of D_0), there is a significant contribution from this term. This contribution decreases as the pathogens diffuse faster (increasing D_0). Moreover, in the limit $D_0 \rightarrow \infty$, this terms tends to zero and (2.33) reduces to the model for well-mixed regime given in equation 5 of [13]. In Sections 3 and 4, the reduced system of ODEs (2.33) is used to compute the basic reproduction number and final size relation for one and two population patches, respectively. The effect of the spatial locations of the patches and their interaction, as characterized by the $O(\nu)$ terms in (2.31), is studied in Section 5.

3. One-patch model

In the previous section, the method of matched asymptotic expansions was used to reduce the dimensionless coupled PDE-ODE model (2.7) to the nonlinear system of ODEs (2.31), for the leading-order density of pathogens p and m population patches. In this section, we consider a single population patch located at the center of a unit disk, and use the dimensionless coupled model (2.7) together with the reduced system of ODEs (2.33) to study the effect of diffusion on the spread of infection in the population.

From (2.7), we derive that the density of pathogens $P(\mathbf{x}, t)$ for this one-patch scenario satisfies

$$\frac{\partial P}{\partial t} = D \Delta P - P, \quad t > 0, \quad \mathbf{x} \in \Omega \setminus \Omega_0; \quad (3.1a)$$

$$\partial_n P = 0, \quad \mathbf{x} \in \partial\Omega; \quad 2\pi\varepsilon D \partial_n P = -\sigma I, \quad \mathbf{x} \in \partial\Omega_0. \quad (3.1b)$$

Here, Ω is a unit disk and $\Omega_0 \subset \Omega$ is a disk of radius $\varepsilon \ll 1$ representing the single population patch, which is located at the center of the unit disk. The density of pathogens P is coupled to the SIR

dynamics of the population given by

$$\begin{aligned}\frac{dS}{dt} &= -\frac{\beta S}{2\pi\varepsilon} \int_{\partial\Omega_0} P \, ds; \\ \frac{dI}{dt} &= \frac{\beta S}{2\pi\varepsilon} \int_{\partial\Omega_0} P \, ds - \phi I; \\ \frac{dR}{dt} &= \phi I,\end{aligned}\tag{3.1c}$$

From the reduced system of ODEs (2.33), we obtain an ODE model for a single population patch given by

$$\frac{dp}{dt} = -p + \frac{1}{|\Omega|}(\sigma I), \quad \frac{dS}{dt} = -\beta S p - \beta S \left(\frac{\sigma I}{2\pi D_0} \right), \quad \frac{dI}{dt} = \beta S p + \beta S \left(\frac{\sigma I}{2\pi D_0} \right) - \phi I, \quad \frac{dR}{dt} = \phi I.\tag{3.2}$$

To study the spread of infection in the population and the effect of diffusion on the epidemic caused by the pathogens, we solve the coupled PDE-ODE model (3.1) numerically using the commercial finite element package, FlexPDE [26] with several different diffusion rates of pathogens. The full PDE results are then compared with results from the reduced system of ODEs (3.2), which is valid for $D = D_0/\nu \gg 1$. In addition, the limiting ODE system (3.2) is analyzed using the method of Kermack-McKendrick similar to that done in [7, 10]. To do so, the following simple lemma is needed:

Lemma 1. *Let $f(t)$ be a nonnegative monotone nonincreasing continuously differentiable function such that as $t \rightarrow \infty$, $f(t) \rightarrow f_\infty \geq 0$, then $f' \rightarrow 0$ as $t \rightarrow \infty$.*

Upon summing the equations for S and I in (3.2), we obtain

$$(S + I)' = -\phi I \leq 0.\tag{3.3}$$

This implies that $(S + I)$ decreases to a limit. It can be shown from Lemma 1 that its derivative approaches zero, so that we can conclude that $I_\infty = \lim_{t \rightarrow \infty} I(t) = 0$. In addition, by integrating (3.3), we obtain

$$\int_0^\infty I(t)dt = \frac{N(0) - S_\infty}{\phi},\tag{3.4}$$

which implies that $\int_0^\infty I(t)dt < \infty$, where $S_\infty = \lim_{t \rightarrow \infty} S(t)$ denotes the total susceptible populations remaining after the outbreak. This simple property is employed when computing the final size relation below.

3.1. The basic reproduction number \mathcal{R}_0

The calculation of the basic reproduction number is done using the next generation matrix method, similar to that done in [14, 27]. Note that there are two infectious classes I and p for this scenario. The Jacobian matrix F for new infections evaluated at the disease free equilibrium state, $\text{DFE}=(S_0, 0, 0)=(N(0), 0, 0)$ is given by

$$F = \left(\frac{\partial \mathcal{F}_i}{\partial x_j} \right)_{i,j} = \begin{pmatrix} \frac{\beta\sigma N(0)}{2\pi D_0} & \beta N(0) \\ 0 & 0 \end{pmatrix},$$

where the functions $\mathcal{F}_1 \equiv dI/dt$, $\mathcal{F}_2 \equiv dp/dt$ in (3.2) and $x_j = I, p$ for $j = 1, 2$. The Jacobian matrix V for transfer of infections between compartments, evaluated at the disease free equilibrium point DFE is

$$V = \left(\frac{\partial \mathcal{V}_i}{\partial x_j} \right)_{i,j} = \begin{pmatrix} \phi & 0 \\ -\frac{\sigma}{|\Omega|} & 1 \end{pmatrix}, \quad \text{and} \quad FV^{-1} = \begin{pmatrix} \frac{\beta N(0)\sigma}{\phi|\Omega|} + \frac{\beta N(0)\sigma}{2\phi\pi D_0} & \beta N(0) \\ 0 & 0 \end{pmatrix}.$$

Remark 1. In order to calculate the basic reproduction number for the model in (3.2), we use the next generation matrix method as in [14, 27] known to be the dominant eigenvalues of FV^{-1} (the spectral radius of the matrix FV^{-1}), and given as

$$\mathcal{R}_0 = \frac{\beta N(0)\sigma}{\phi|\Omega|} + \frac{\beta N(0)\sigma}{2\phi\pi D_0}. \quad (3.5)$$

Conveniently, we can decompose \mathcal{R}_0 as $\mathcal{R}_0 = \mathcal{R}_\star + \mathcal{R}_D$, where $\mathcal{R}_\star = \frac{\beta N(0)\sigma}{\phi|\Omega|}$ and $\mathcal{R}_D = \frac{\beta N(0)\sigma}{2\phi\pi D_0}$.

The expression for \mathcal{R}_0 in (3.5) denotes the secondary infections contributed by indirect transmission (\mathcal{R}_\star) and diffusion (\mathcal{R}_D). The term \mathcal{R}_\star represents the secondary infections caused indirectly through the pathogen since a single infective I sheds a quantity σ of the pathogen per unit time for a time period $1/\phi$ and this pathogen infects βN susceptibles. The second term \mathcal{R}_D denotes the secondary infections caused by the pathogen diffusing in the bulk at the rate D_0 since a single infective I sheds a quantity σ of the pathogen per unit time for a time period $1/\phi$ and this pathogen infects βN susceptible individuals in the patch. As the diffusion rate of pathogens become asymptotically large, that is, $D_0 \rightarrow \infty$, we observe that $\mathcal{R}_D \rightarrow 0$. Therefore, in this limit, the basic reproduction number \mathcal{R}_0 in (3.5) can be written as

$$\mathcal{R}_0^\infty = \lim_{D_0 \rightarrow \infty} \mathcal{R}_0 = \frac{\beta N(0)\sigma}{\phi|\Omega|} = \mathcal{R}_\star. \quad (3.6)$$

A more detailed discussion of equation (3.6) will be given below while explaining our numerical simulations. The implication of the basic reproduction number \mathcal{R}_0 is summarized as follows in the readily proved result.

Theorem 1. For system (3.2), the infection dies out whenever $\mathcal{R}_0 < 1$. In contrast, an epidemic occurs whenever $\mathcal{R}_0 > 1$.

3.2. The final size relation

The final size relation gives an estimate of the total number of infections and the epidemic size for the period of the epidemic in terms of the parameters in the model, as similar to that done in [3, 5]. In other words, the final size relation is used to estimate the total number of disease deaths and cases from the parameters of the model. Following the approach in [1, 4, 5, 7, 6, 8, 9, 11], we integrate the equation for S in (3.2) to get

$$\log \frac{S_0}{S_\infty} = \beta \int_0^\infty p(t)dt + \frac{\beta\sigma}{2\pi D_0} \int_0^\infty I(t)dt, \quad (3.7)$$

Similarly, integrating the equation for $p(t)$ in (3.2) gives

$$p(t) = p_0 e^{-t} + \frac{\sigma}{|\Omega|} \int_0^t e^{-(t-s)} I(s) ds. \quad (3.8)$$

Next, we need to show that

$$\lim_{t \rightarrow \infty} \int_0^t e^{-(t-s)} I(s) ds = \lim_{t \rightarrow \infty} \frac{\int_0^t e^s I(s) ds}{e^t} = 0. \quad (3.9)$$

If the integral in the numerator of (3.9) is bounded, this relation is immediate. If the numerator is unbounded, L'Hopital's rule yields that $\lim_{t \rightarrow \infty} \int_0^t e^{-(t-s)} I(s) ds = \lim_{t \rightarrow \infty} I(t) = I(\infty)$, which vanishes as established above following equation (3.3). Therefore, (3.8) yields that

$$p_\infty = \lim_{t \rightarrow \infty} p(t) = 0.$$

By integrating (3.8), interchanging the order of integration, and then using (3.4), we get

$$\int_0^\infty p(t) dt = \frac{\sigma}{|\Omega|} \int_0^\infty I(t) dt + p_0, \quad (3.10)$$

which implies that $\int_0^\infty p(t) dt < \infty$. Upon substituting (3.10) into (3.7), we obtain

$$\log \frac{S_0}{S_\infty} = \frac{\beta\sigma}{|\Omega|} \int_0^\infty I(t) dt + \frac{\beta\sigma}{2\pi D_0} \int_0^\infty I(t) dt + \beta p_0,$$

so that, by using (3.4), we obtain the final size relation

$$\begin{aligned} \log \frac{S_0}{S_\infty} &= \frac{\beta\sigma N}{\phi|\Omega|} \left\{ 1 - \frac{S_\infty}{N} \right\} + \frac{\beta\sigma N}{2\pi\phi D_0} \left\{ 1 - \frac{S_\infty}{N} \right\} + \beta p_0, \\ &= \mathcal{R}_\star \left\{ 1 - \frac{S_\infty}{N} \right\} + \mathcal{R}_D \left\{ 1 - \frac{S_\infty}{N} \right\} + \beta p_0. \end{aligned}$$

This implies that $S_\infty > 0$. In a situation where the outbreak begins with no contact with pathogen, so that $p_0 = 0$, the final size relation becomes

$$\log \frac{S_0}{S_\infty} = \mathcal{R}_\star \left\{ 1 - \frac{S_\infty}{N} \right\} + \mathcal{R}_D \left\{ 1 - \frac{S_\infty}{N} \right\} = (\mathcal{R}_\star + \mathcal{R}_D) \left\{ 1 - \frac{S_\infty}{N} \right\} = \mathcal{R}_0 \left\{ 1 - \frac{S_\infty}{N} \right\}. \quad (3.11)$$

Equation (3.11) is referred to as the *final size relation*, and this gives a relationship between the basic reproduction number and the epidemic size. Note that the total number of infected population over the period of the epidemic is $N - S_\infty$ and can also be described in terms of the attack rate $(1 - S_\infty/N)$ as in [5].

3.3. Numerical simulation for one-patch model

Next, we present some numerical simulations of the coupled PDE-ODE model (3.1) and the reduced system of ODEs (3.2) for the case of a single population patch located at the center of a unit disk. The coupled model (3.1) is solved numerically using the commercial finite element package FlexPDE [26],

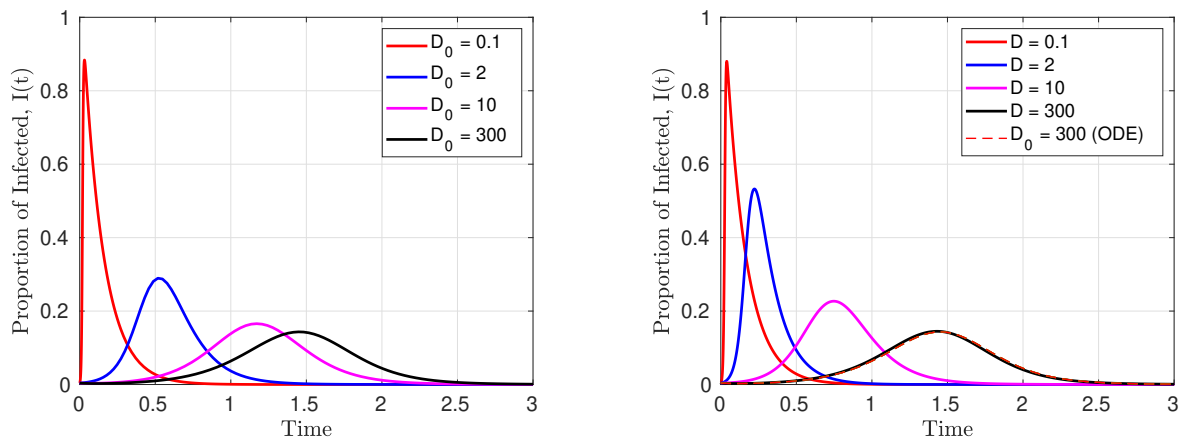
Table 1. Model Variables and their Descriptions

Parameter	Description	Dimensional(less) values
μ (β)	dimensional (dimensionless) effective contact rate	0.3 [3] (computed using (2.8))
r (σ)	dimensional (dimensionless) pathogen shedding rate	0.1 [30] (computed using (2.8))
α (ϕ)	dimensional (dimensionless) removed rate for infected individuals	1.87 [30] (computed using (2.8))
δ	dimensional decay rate of pathogens	0.25
p_c	typical value for density of pathogens	0.01
ε	radius of the population patches	0.02
$ \Omega $	area of the domain (unit disk)	π

while the reduce ODE system (3.2) is solved using the numerical ODE solver *ODE45* in MATLAB [25]. For these models, simulations are done with different diffusion rates of pathogens in order to understand the effect of diffusion on the dynamics of the infected population. The parameters used for these simulations are shown in Table 1.

Figure 1 shows the proportion of infected over time when an epidemic begins with one infective in a total population of 250 individuals, with susceptible, infected and recovered population given as $S(0) = 249/250$, $I(0) = 1/250$ and $R(0) = 0$, respectively. The initial density of pathogen used for both the coupled model and the reduced system of ODEs is $p(0) = P(0) = 0$, denoting that the outbreak begins with no pathogen in the air, and that the only source of pathogen into the system is the ones shed by infected individuals. We observe from this figure that the proportion of infected individuals decreases with increases in the diffusion rate of pathogen. This shows that when pathogens diffuse slowly, they cluster around the population as they are being shed. As a result, since human populations are confined in a region, this in turn leads to more infections.

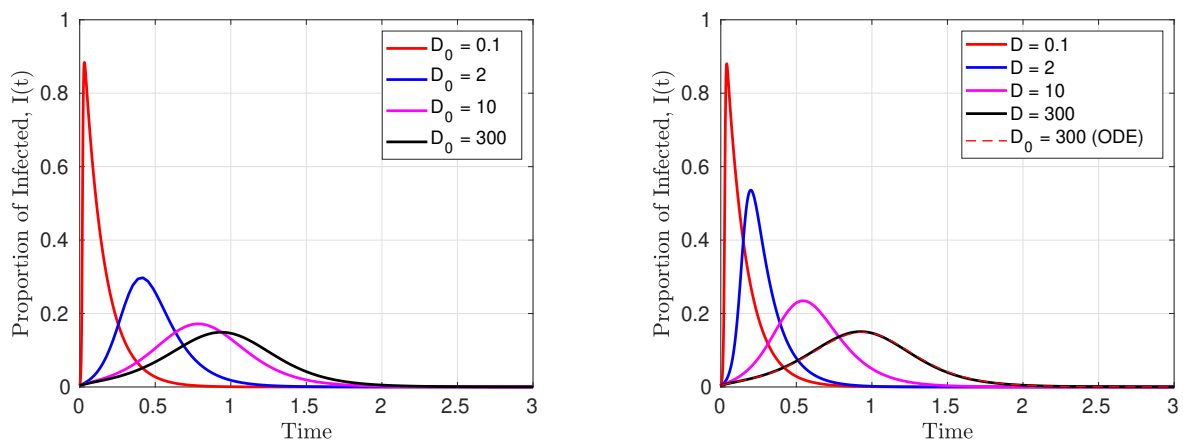
However, when pathogens diffuse faster (diffusion rate increases), they diffuse away from the population as they are being shed, which in turn, reduces the density of pathogens around the patch. This effect lowers the population of infected individuals. Comparing Figure 1(a) and 1(b), we notice that the proportion of infectives estimated by the two models are similar when D and D_0 are small and when they are asymptotically large. Since $D = D_0/\nu$, a small value of D_0 implies that D is also small. As a result of this, the two models would behave similar in this limit even though the reduced system of ODEs (3.2) is only valid in the limit $D = \mathcal{O}(\nu^{-1})$, where $\nu = -\log \varepsilon$, with $\varepsilon \ll 1$. The difference between the two models becomes more apparent with an increase in the diffusion rate, as the number of infectives estimated by the system of ODEs is less as compared to that of the PDE-ODE model. This is because the system of ODEs is valid in the limit $D = \mathcal{O}(\nu^{-1})$, and the spread of infection decreases as D increases. Lastly, as the diffusion rates become asymptotically large, the solutions of the two models essentially coincide. This is because when $D \rightarrow \infty$, the problem becomes well-mixed, where the density of pathogen is homogeneous in space, and the coupled PDE-ODE model can be reduced to a system of ODEs. Similarly, if we take the limit of the reduced system of ODEs (3.2) as $D_0 \rightarrow \infty$, we have the model studied in [7]. This suggests that the model in [7] can be interpreted as the well-mixed limit of the coupled PDE-ODE model (3.1).



(a) Simulation of the reduced system of ODE (3.2)

(b) Simulation of the coupled PDE-ODE (3.1)

Figure 1. The dynamics of infected $I(t)$ for different diffusion rates of pathogen D and D_0 , and other parameters as in Table 1. (a) shows the result obtained from the system of ODEs (3.2) with initial conditions $(S(0), I(0), R(0), p(0)) = (249/250, 1/250, 0, 0)$, while (b) is the result of the dimensionless coupled PDE-ODE model (3.1) with initial conditions $(S(0), I(0), R(0), P(0)) = (249/250, 1/250, 0, 0)$.



(a) Simulation of the reduced system of ODE (3.2)

(b) Simulation of the coupled PDE-ODE (3.1)

Figure 2. The dynamics of proportion of infected individuals $I(t)$ for different diffusion rates of pathogen, and all other parameters as in Table 1. (a) shows the result obtained from the system of ODEs (3.2) with initial conditions $(S(0), I(0), R(0), p(0)) = (249/250, 1/250, 0, 1)$, while (b) is the result of the dimensionless coupled PDE-ODE model (3.1) with initial conditions $(S(0), I(0), R(0), P(0)) = (249/250, 1/250, 0, 1)$.

The results in Figure 2 are similar to those in Figure 1 except that the initial conditions of the pathogens is taken as $P(0) = p(0) = 1$. This models the case where there is pathogen in the air at the beginning of the outbreak. The other initial conditions are the same as those used in Figure 1. These results show how the presence of pathogens in the atmosphere at the beginning of the outbreak would affect the transmission of infection. The epidemic takes off earlier when there are pathogens in the air at the beginning of the outbreak (Figure 2) compared to when there are no pathogens at the beginning (Figure 1). When the diffusion rate is small, the model with (Figure 2) and without (Figure 1) pathogen at the beginning of the outbreak have similar estimates. This is because the pathogens are barely moving when the diffusion rate is small, and as a result, it does not make much difference whether they are present or not. As the diffusion rate of pathogens increases, there seems to be significant differences in the two solutions, since, the epidemic takes off earlier in Figure 2 as compared to Figure 1. Therefore, the presence of pathogens in the air around the population patch increases the spread of infection in the population, as expected intuitively.

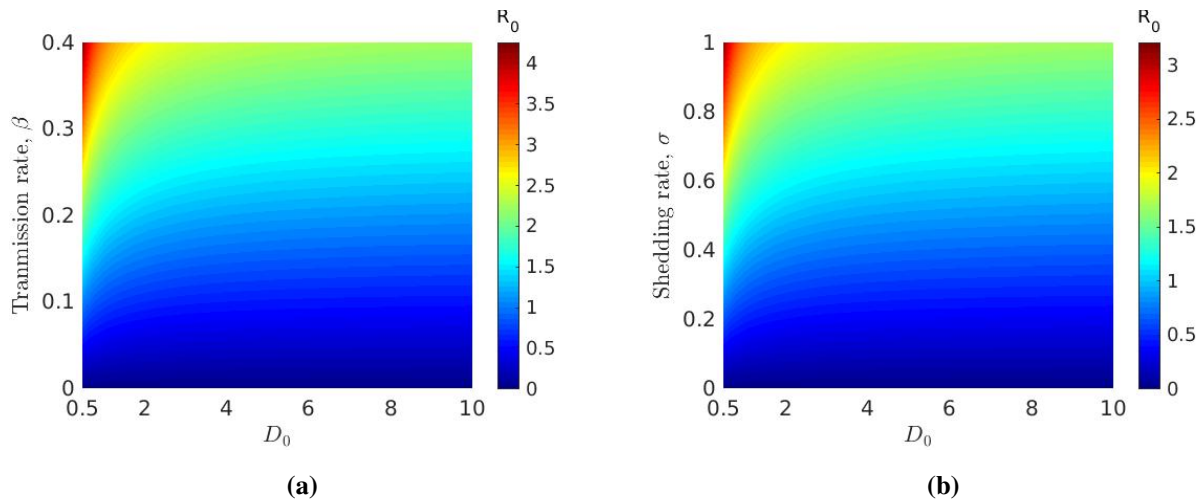


Figure 3. Surface plots of the basic reproduction number \mathcal{R}_0 in (3.5) for the one-patch model (3.2) plotted with respect to the diffusion rate of pathogens D_0 and some dimensionless parameters of the SIR model. (a) is for D_0 and the transmission rate β , while (b) is for D_0 and the shedding rate σ . The parameters used are given in Table 1.

The surface plots in Figure 3 show the basic reproduction number \mathcal{R}_0 in (3.5) for the one-patch model (3.2) in terms of the diffusion rate of pathogens D_0 and the dimensionless transmission and shedding rates, β and σ , respectively. These results show the effect of D_0 on the basic reproduction number, \mathcal{R}_0 . We observe from both results in this figure that \mathcal{R}_0 increases as the transmission and shedding rates increase, and decreases as D_0 increases for a fixed value of the transmission and shedding rates. These results agree with the simulations in Figures 1 and 2, where the spread of infections decreases as the diffusion rate of pathogen increases. In Figure 3(a), the largest \mathcal{R}_0 is obtained when D_0 is small and the transmission rate β is large. This is reasonable because when pathogens diffuse slowly, it would take longer for them to diffuse away from the population, and as a result, they continue to cause infections in the population, and consequently this leads to a large basic reproduction number. Similarly, in Figure 3(b), the largest \mathcal{R}_0 is obtained when the shedding rate of pathogen is large and D_0 is small, because when infected individuals shed pathogens at a high rate and the pathogens do not

diffuse away from the population, they lead to more infections. When the transmission and shedding rates are low, irrespective of the diffusion rate of pathogens, the reproduction number will be less than one and the epidemic will die out.

In the next section, we perform a similar analysis for a scenario with two spatially segregated population patches.

4. Two-patch model

In the previous section, we studied the effect of the diffusion rate of pathogens on the spread of infection in a single population. In this section, we consider a scenario with two population patches, and use the dimensionless coupled PDE-ODE model (2.7) and the reduced system of ODEs (2.33) with $m = 2$ to study the dynamics of infection in these populations. The patches are centered at $\mathbf{x}_1 = (0.5, 0)$ and $\mathbf{x}_2 = (-0.5, 0)$ in a unit disk.

For this two-patch scenario, the density of pathogen P for the coupled PDE-ODE model satisfies

$$\frac{\partial P}{\partial t} = D \Delta P - P, \quad t > 0, \quad \mathbf{x} \in \Omega \setminus \{\Omega_1 \cup \Omega_2\}; \quad (4.1a)$$

$$\partial_n P = 0, \quad \mathbf{x} \in \partial\Omega; \quad 2\pi\varepsilon D \partial_n P = -\sigma_1 I_1, \quad \mathbf{x} \in \partial\Omega_1; \quad 2\pi\varepsilon D \partial_n P = -\sigma_2 I_2, \quad \mathbf{x} \in \partial\Omega_2, \quad (4.1b)$$

where Ω_1 and Ω_2 are the two population patches centered at $\mathbf{x}_1 = (0.5, 0)$ and $\mathbf{x}_2 = (-0.5, 0)$. This density of pathogen is coupled to the population dynamics of the two patches through the following ODE system:

Patch 1	Patch 2
$\frac{dS_1}{dt} = -\frac{\beta_1 S_1}{2\pi\varepsilon} \int_{\partial\Omega_1} P \, ds;$	$\frac{dS_2}{dt} = -\frac{\beta_2 S_2}{2\pi\varepsilon} \int_{\partial\Omega_2} P \, ds;$
$\frac{dI_1}{dt} = \frac{\beta_1 S_1}{2\pi\varepsilon} \int_{\partial\Omega_1} P \, ds - \phi_1 I_1;$	$\frac{dI_2}{dt} = \frac{\beta_2 S_2}{2\pi\varepsilon} \int_{\partial\Omega_2} P \, ds - \phi_2 I_2;$
$\frac{dR_1}{dt} = \phi_1 I_1;$	$\frac{dR_2}{dt} = \phi_2 I_2.$

(4.1c)

The coupled PDE-ODE model (4.1) is solved numerically using FlexPDE [26] with different diffusion rates for the pathogens. The solutions are used to study the effect of diffusion on the spread of the infection caused by the pathogens within the population. From (2.33), we construct the reduced system of ODEs for the case of two patches as

$$\frac{dp}{dt} = -p + \frac{1}{|\Omega|}(\sigma_1 I_1 + \sigma_2 I_2), \quad (4.2a)$$

Patch 1	Patch 2
$\frac{dS_1}{dt} = -\beta_1 S_1 p - \beta_1 S_1 \left(\frac{\sigma_1 I_1}{2\pi D_0} \right),$	$\frac{dS_2}{dt} = -\beta_2 S_2 p - \beta_2 S_2 \left(\frac{\sigma_2 I_2}{2\pi D_0} \right),$
$\frac{dI_1}{dt} = \beta_1 S_1 p + \beta_1 S_1 \left(\frac{\sigma_1 I_1}{2\pi D_0} \right) - \phi_1 I_1,$	$\frac{dI_2}{dt} = \beta_2 S_2 p + \beta_2 S_2 \left(\frac{\sigma_2 I_2}{2\pi D_0} \right) - \phi_2 I_2,$

(4.2b)

$$\frac{dR_1}{dt} = \phi_1 I_1, \quad \frac{dR_2}{dt} = \phi_2 I_2,$$

with initial conditions

$$S_1(0) = S_{10}, \quad S_2(0) = S_{20}, \quad I_1(0) = I_{10}, \quad I_2(0) = I_{20}, \quad R_1(0) = 0, \quad R_2(0) = 0, \quad p(0) = p_0,$$

in a population of constant total size $N = N_1 + N_2$, where $N_1 = S_1 + I_1 + R_1 = S_{10} + I_{10}$ and $N_2 = S_2 + I_2 + R_2 = S_{20} + I_{20}$. This system of ODEs is similar to the model studied in [13], in which indirect transmission of diseases with no diffusion was studied. For our model we will compute the basic reproduction number and the final size relation. The analytical approach for the Kermack-McKendrick epidemic model, as employed in [7] and [10], will be used in the analysis.

Summing the equations for S_1 and I_1 , and then those for S_2 and I_2 in (4.2b), we obtain

$$(S_1 + I_1)' = -\phi_1 I_1 \leq 0. \quad (4.3)$$

$$(S_2 + I_2)' = -\phi_2 I_2 \leq 0. \quad (4.4)$$

Here, we see that $(S_1 + I_1)$ and $(S_2 + I_2)$ decreases to a limit, and we can show from Lemma 1 that their derivatives approach zero. Therefore, we conclude that $I_{1\infty} = \lim_{t \rightarrow \infty} I_1(t) = 0$ and $I_{2\infty} = \lim_{t \rightarrow \infty} I_2(t) = 0$.

Next, by integrating (4.3) we get $\phi_1 \int_0^\infty I_1(t) dt = S_1(0) + I_1(0) - S_{1\infty} = N_1(0) - S_{1\infty}$, so that

$$\int_0^\infty I_1(t) dt = \frac{N_1(0) - S_{1\infty}}{\phi_1}, \quad (4.5)$$

which implies that $\int_0^\infty I_1(t) dt < \infty$. Similarly, we integrate (4.4), to obtain

$$\int_0^\infty I_2(t) dt = \frac{N_2(0) - S_{2\infty}}{\phi_2}. \quad (4.6)$$

Here, $S_{1\infty} = \lim_{t \rightarrow \infty} S_1(t)$ and $S_{2\infty} = \lim_{t \rightarrow \infty} S_2(t)$ denote the total susceptible population remaining after the outbreak in patch 1 and patch 2, respectively.

4.1. Reproduction number \mathcal{R}_0

Following a similar approach to that used in Section 3.1 for the one-patch model, we construct our system of infected classes as

$$\frac{dI_1}{dt} = \beta_1 S_1 p + \beta_1 S_1 \left(\frac{\sigma_1 I_1}{2\pi D_0} \right) - \phi_1 I_1, \quad (4.7a)$$

$$\frac{dI_2}{dt} = \beta_2 S_2 p + \beta_2 S_2 \left(\frac{\sigma_2 I_2}{2\pi D_0} \right) - \phi_2 I_2, \quad (4.7b)$$

$$\frac{dp}{dt} = -p + \frac{1}{|\Omega|} (\sigma_1 I_1 + \sigma_2 I_2). \quad (4.7c)$$

Using the next generation matrix approach in [14], [27], the basic reproduction number is calculated as follows. We first introduce the three infectious classes I_1, I_2, p , and

the Jacobian matrix of $\mathcal{F}_i = (\mathcal{F}_1, \mathcal{F}_2, \mathcal{F}_3)$, evaluated at the disease free equilibrium point $\text{DFE}=(S_{10}, 0, 0, S_{20}, 0, 0)=(N_1(0), 0, 0, N_2(0), 0, 0)$ given by

$$F = \left(\frac{\partial \mathcal{F}_i}{\partial x_j} \right)_{i,j} = \begin{pmatrix} \frac{\beta_1 \sigma_1 N_1(0)}{2\pi D_0} & 0 & \beta_1 N_1(0) \\ 0 & \frac{\beta_2 \sigma_2 N_2(0)}{2\pi D_0} & \beta_2 N_2(0) \\ 0 & 0 & 0 \end{pmatrix},$$

where $x_j = I_1, I_2, p$ for $j = 1, 2, 3$ and $i = 1, 2, 3$.

The Jacobian matrix of $\mathcal{V}_i = (\mathcal{V}_1, \mathcal{V}_2, \mathcal{V}_3)$, evaluated at the disease free equilibrium point DFE is

$$V = \left(\frac{\partial \mathcal{V}_i}{\partial x_j} \right)_{i,j} = \begin{pmatrix} \phi_1 & 0 & 0 \\ 0 & \phi_2 & 0 \\ -\frac{\sigma_1}{|\Omega|} & -\frac{\sigma_2}{|\Omega|} & 1 \end{pmatrix}, \quad \text{and}$$

$$FV^{-1} = \begin{pmatrix} \frac{\beta_1 N_1(0)\sigma_1}{\phi_1|\Omega|} + \frac{\beta_1 N_1(0)\sigma_1}{2\phi_1\pi D_0} & \frac{\beta_1 N_1(0)\sigma_2}{\phi_2|\Omega|} & \beta_1 N_1(0) \\ \frac{\beta_2 N_2(0)\sigma_1}{\phi_1|\Omega|} & \frac{\beta_2 N_2(0)\sigma_2}{\phi_2|\Omega|} + \frac{\beta_2 N_2(0)\sigma_2}{2\phi_2\pi D_0} & \beta_2 N_2(0) \\ 0 & 0 & 0 \end{pmatrix}.$$

Remark 2. To calculate the basic reproduction number for the 2-patch model in (4.7), we use the method of next generation matrix in [14, 27] given as the dominant eigenvalues of FV^{-1} (the spectral radius of the matrix FV^{-1}). A simple calculation yields that

$$\mathcal{R}_0 = \frac{(|\Omega| + 2\pi D_0)\clubsuit}{4\pi\phi_1\phi_2|\Omega|D_0} + \frac{\sqrt{(|\Omega|^2 + 4\pi|\Omega|D_0)\spadesuit^2 + 4\pi^2 D_0^2 \clubsuit^2}}{4\pi\phi_1\phi_2|\Omega|D_0}, \quad (4.8)$$

where we have defined \clubsuit and \spadesuit by

$$\clubsuit = \beta_1 N_1(0)\phi_2\sigma_1 + \beta_2 N_2(0)\phi_1\sigma_2, \quad \spadesuit = \beta_1 N_1(0)\phi_2\sigma_1 - \beta_2 N_2(0)\phi_1\sigma_2.$$

In the well-mixed limit $D_0 \gg 1$, similar to that studied for the one patch model in Section 3, the reproduction number \mathcal{R}_0 in (4.8) reduces to $\mathcal{R}_0^\infty = \lim_{D_0 \rightarrow \infty} \mathcal{R}_0 = \clubsuit/(\phi_1\phi_2|\Omega|)$, which implies that

$$\mathcal{R}_0^\infty = \frac{\beta_1 N_1(0)\sigma_1}{\phi_1|\Omega|} + \frac{\beta_2 N_2(0)\sigma_2}{\phi_2|\Omega|}. \quad (4.9)$$

We observe that \mathcal{R}_0^∞ can also be decomposed as $\mathcal{R}_0^\infty = \beta_1 \mathcal{R}_1 + \beta_2 \mathcal{R}_2$, where $\mathcal{R}_1 = \frac{N_1(0)\sigma_1}{\phi_1|\Omega|}$ and $\mathcal{R}_2 = \frac{N_2(0)\sigma_2}{\phi_2|\Omega|}$.

We can interpret the large D_0 limiting value \mathcal{R}_0^∞ of the reproduction number as follows. The formula for \mathcal{R}_0^∞ in (4.9) denotes the contribution of the first and second patch. The term $\beta_1 \mathcal{R}_1$ represents the secondary infections caused indirectly through the pathogen since a single infective I_1 sheds a quantity σ_1 of the pathogen per unit time for a time period $1/\phi_1$, and this pathogen infects $\beta_1 N_1$ susceptibles. The second term $\beta_2 \mathcal{R}_2$ denotes the secondary infections caused indirectly through the pathogen since a single infective I_2 sheds a quantity σ_2 of the pathogen per unit time for a time period $1/\phi_2$, and this pathogen infects $\beta_2 N_2$ susceptibles.

A detailed qualitative explanation of \mathcal{R}_0 (for the case where $D_0 = \mathcal{O}(1)$) and \mathcal{R}_0^∞ (for the well-mixed limit $D_0 \rightarrow \infty$), will be given below when discussing our results from numerical simulations. The following easily-proved Theorem summarizes the implications of the reproduction number \mathcal{R}_0^∞ .

Theorem 2. *For the well-mixed limit $D_0 \rightarrow \infty$ for the system (4.2), the infection dies out whenever $\mathcal{R}_0^\infty < 1$, while an epidemic occurs whenever $\mathcal{R}_0^\infty > 1$.*

4.2. The final size relation

Following the same approach as in subsection 3.2, we integrate the equations for S_1 and S_2 in (4.2b) to get

$$\log \frac{S_{10}}{S_{1\infty}} = \beta_1 \int_0^\infty p(t) dt + \frac{\beta_1 \sigma_1}{2\pi D_0} \int_0^\infty I_1(t) dt, \quad (4.10)$$

and

$$\log \frac{S_{20}}{S_{2\infty}} = \beta_2 \int_0^\infty p(t) dt + \frac{\beta_2 \sigma_2}{2\pi D_0} \int_0^\infty I_2(t) dt. \quad (4.11)$$

Similarly, integrating the equation for p in (4.2a), we obtain

$$p(t) = p_0 e^{-t} + \frac{\sigma_1}{|\Omega|} \int_0^t e^{-(t-s)} I_1(s) ds + \frac{\sigma_2}{|\Omega|} \int_0^t e^{-(t-s)} I_2(s) ds. \quad (4.12)$$

Next, we need to show that

$$\lim_{t \rightarrow \infty} \int_0^t e^{-(t-s)} I_1(s) ds = \lim_{t \rightarrow \infty} \frac{\int_0^t e^s I_1(s) ds}{e^t} = 0 \quad \text{and} \quad \lim_{t \rightarrow \infty} \int_0^t e^{-(t-s)} I_2(s) ds = \lim_{t \rightarrow \infty} \frac{\int_0^t e^s I_2(s) ds}{e^t} = 0. \quad (4.13)$$

If the integral in the numerators of the two expressions in (4.13) are bounded, the result is immediate. Alternatively, if these integrals are unbounded, then by L'Hopital's rule these two limits reduce to $\lim_{t \rightarrow \infty} I_1(t)$ and $\lim_{t \rightarrow \infty} I_2(t) = 0$, which vanish since $I_1(\infty) = I_2(\infty) = 0$ as was shown above following (4.4) (see also [7]). As a result, (4.12) yields that

$$p_\infty = \lim_{t \rightarrow \infty} p(t) = 0.$$

Next, upon integrating (4.12), interchanging the order of integration, and then using (4.5) and (4.6), we get

$$\int_0^\infty p(t) dt = p_0 + \frac{\sigma_1}{|\Omega|} \int_0^\infty I_1(t) dt + \frac{\sigma_2}{|\Omega|} \int_0^\infty I_2(t) dt, \quad (4.14)$$

which implies that $\int_0^\infty p(t) dt < \infty$.

We then substitute (4.14) into (4.10) and (4.11) to get

$$\log \frac{S_{10}}{S_{1\infty}} = \frac{\beta_1 \sigma_1}{|\Omega|} \int_0^\infty I_1(t) dt + \frac{\beta_1 \sigma_2}{|\Omega|} \int_0^\infty I_2(t) dt + \frac{\beta_1 \sigma_1}{2\pi D_0} \int_0^\infty I_1(t) dt + \beta_1 p_0,$$

and

$$\log \frac{S_{20}}{S_{2\infty}} = \frac{\beta_2 \sigma_1}{|\Omega|} \int_0^\infty I_1(t) dt + \frac{\beta_2 \sigma_2}{|\Omega|} \int_0^\infty I_2(t) dt + \frac{\beta_2 \sigma_2}{2\pi D_0} \int_0^\infty I_2(t) dt + \beta_2 p_0,$$

which yields the final size relation

$$\log \frac{S_{10}}{S_{1\infty}} = \frac{\beta_1 \sigma_1 N_1(0)}{\phi_1 |\Omega|} \left\{ 1 - \frac{S_{1\infty}}{N_1(0)} \right\} + \frac{\beta_1 \sigma_2 N_2(0)}{\phi_2 |\Omega|} \left\{ 1 - \frac{S_{2\infty}}{N_2(0)} \right\} + \frac{\beta_1 \sigma_1 N_1(0)}{2\pi \phi_1 D_0} \left\{ 1 - \frac{S_{1\infty}}{N_1(0)} \right\} + \beta_1 p_0,$$

and

$$\log \frac{S_{20}}{S_{2\infty}} = \frac{\beta_2 \sigma_1 N_1(0)}{\phi_1 |\Omega|} \left\{ 1 - \frac{S_{1\infty}}{N_1(0)} \right\} + \frac{\beta_2 \sigma_2 N_2(0)}{\phi_2 |\Omega|} \left\{ 1 - \frac{S_{2\infty}}{N_2(0)} \right\} + \frac{\beta_2 \sigma_2 N_2(0)}{2\pi \phi_2 D_0} \left\{ 1 - \frac{S_{2\infty}}{N_2(0)} \right\} + \beta_2 p_0.$$

These expressions can be written by using $\mathcal{R}_1 = \frac{N_1(0)\sigma_1}{\phi_1 |\Omega|}$ and $\mathcal{R}_2 = \frac{N_2(0)\sigma_2}{\phi_2 |\Omega|}$, as

$$\log \frac{S_{10}}{S_{1\infty}} = \beta_1 \left(\mathcal{R}_1 \left\{ 1 - \frac{S_{1\infty}}{N_1(0)} \right\} + \mathcal{R}_2 \left\{ 1 - \frac{S_{2\infty}}{N_2(0)} \right\} + \frac{\sigma_1 N_1(0)}{2\pi \phi_1 D_0} \left\{ 1 - \frac{S_{1\infty}}{N_1(0)} \right\} \right) + \beta_1 p_0,$$

and

$$\log \frac{S_{20}}{S_{2\infty}} = \beta_2 \left(\mathcal{R}_1 \left\{ 1 - \frac{S_{1\infty}}{N_1(0)} \right\} + \mathcal{R}_2 \left\{ 1 - \frac{S_{2\infty}}{N_2(0)} \right\} + \frac{\sigma_2 N_2(0)}{2\pi \phi_2 D_0} \left\{ 1 - \frac{S_{2\infty}}{N_2(0)} \right\} \right) + \beta_2 p_0,$$

where we used (4.3), which implies $S_{1\infty} > 0$ and $S_{2\infty} > 0$. In the case where the outbreak begins with no contact with pathogen, so that $p_0 = 0$, the *final size relation* for patch 1 and 2 can be written as

$$\log \frac{S_{10}}{S_{1\infty}} = \beta_1 \left(\mathcal{R}_1 \left\{ 1 - \frac{S_{1\infty}}{N_1(0)} \right\} + \mathcal{R}_2 \left\{ 1 - \frac{S_{2\infty}}{N_2(0)} \right\} + \frac{\sigma_1 N_1(0)}{2\pi \phi_1 D_0} \left\{ 1 - \frac{S_{1\infty}}{N_1(0)} \right\} \right), \quad (4.15)$$

$$\log \frac{S_{20}}{S_{2\infty}} = \beta_2 \left(\mathcal{R}_1 \left\{ 1 - \frac{S_{1\infty}}{N_1(0)} \right\} + \mathcal{R}_2 \left\{ 1 - \frac{S_{2\infty}}{N_2(0)} \right\} + \frac{\sigma_2 N_2(0)}{2\pi \phi_2 D_0} \left\{ 1 - \frac{S_{2\infty}}{N_2(0)} \right\} \right).$$

In the well-mixed limit of asymptotically large diffusion in which $D_0 \rightarrow \infty$, the final size relation (4.15) becomes

$$\begin{aligned} \log \frac{S_{10}}{S_{1\infty}} &= \beta_1 \left(\mathcal{R}_1 \left\{ 1 - \frac{S_{1\infty}}{N_1(0)} \right\} + \mathcal{R}_2 \left\{ 1 - \frac{S_{2\infty}}{N_2(0)} \right\} \right), \\ \log \frac{S_{20}}{S_{2\infty}} &= \beta_2 \left(\mathcal{R}_1 \left\{ 1 - \frac{S_{1\infty}}{N_1(0)} \right\} + \mathcal{R}_2 \left\{ 1 - \frac{S_{2\infty}}{N_2(0)} \right\} \right). \end{aligned} \quad (4.16)$$

This result can be written in matrix form as

$$\begin{pmatrix} \log \frac{S_{10}}{S_{1\infty}} \\ \log \frac{S_{20}}{S_{2\infty}} \end{pmatrix} = \begin{pmatrix} \mathbb{T}_{11} & \mathbb{T}_{12} \\ \mathbb{T}_{21} & \mathbb{T}_{22} \end{pmatrix} \begin{pmatrix} 1 - \frac{S_{1\infty}}{N_1(0)} \\ 1 - \frac{S_{2\infty}}{N_2(0)} \end{pmatrix}, \quad \text{where} \quad \mathbb{T} = \begin{pmatrix} \beta_1 \mathcal{R}_1 & \beta_1 \mathcal{R}_2 \\ \beta_2 \mathcal{R}_1 & \beta_2 \mathcal{R}_2 \end{pmatrix}. \quad (4.17)$$

Note that the total number of infected populations in patch 1 and 2 over the period of the epidemic are respectively $N_1 - S_{1\infty}$ and $N_2(0) - S_{2\infty}$, and can be described in terms of the attack rate $(1 - S_{1\infty}/N_1(0))$ and $(1 - S_{2\infty}/N_2(0))$ as in [5].

4.3. Numerical simulation for two-patch model

Here, we present numerical simulations of the dimensional coupled PDE-ODE model (4.1) and the reduced system of ODEs (4.2) for the case of two population patches. Our goal is to study the spread of infection between and within these populations. For the coupled PDE-ODE model, our patches are centered at $\mathbf{x}_1 = (0.5, 0)$ and $\mathbf{x}_2 = (-0.5, 0)$ for patches 1 and 2, respectively.

The results in Figure 4 show the proportion of infected individuals for the two patches in the case where the outbreak begins with no pathogen in the air ($P(0) = p(0) = 0$), only one infected individual in patch 1 ($I_1(0) = 1/250$), and no infections in patch 2 ($I_2(0) = 0$). The population patches are assumed to be identical with parameters as given in Table 2.

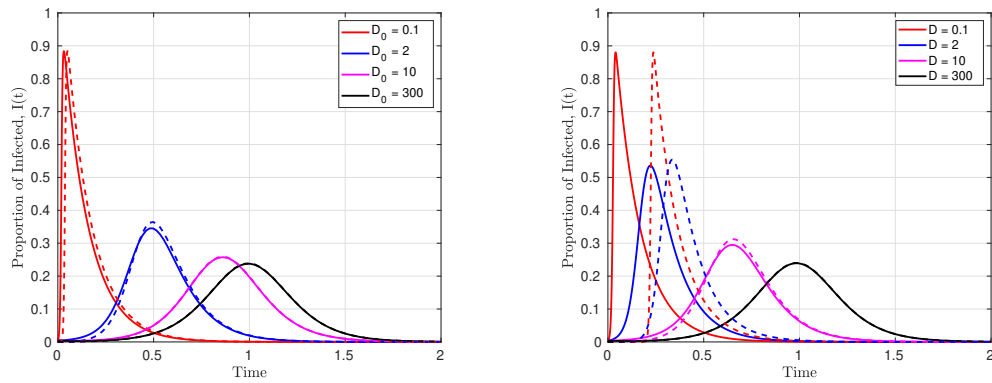
Table 2. Parameter Descriptions and Values for the Two-Patch Model.

Parameter	Description	Patch 1, 2 values
μ (β)	dimensional (dimensionless) effective contact rate	0.3, 1.2 [3] (computed using (2.8))
r (σ)	dimensional (dimensionless) pathogen shedding rate	0.1, 1 [30] (computed using (2.8))
α (ϕ)	dimensional (dimensionless) removed rate for infected individuals	1.87 [30] (computed using (2.8))
N_1, N_2	total population	300, 250
δ	dimensionless decay rate of pathogens	0.25
p_c	typical value for density of pathogens	0.01
ε	radius of the population patch	0.02
$ \Omega $	area of the domain (unit disk)	π

Figures 4(a) and 4(b) show the result obtained from the reduced system of ODEs (4.2) and the coupled PDE-ODE model (4.1) respectively, for different diffusion rates.

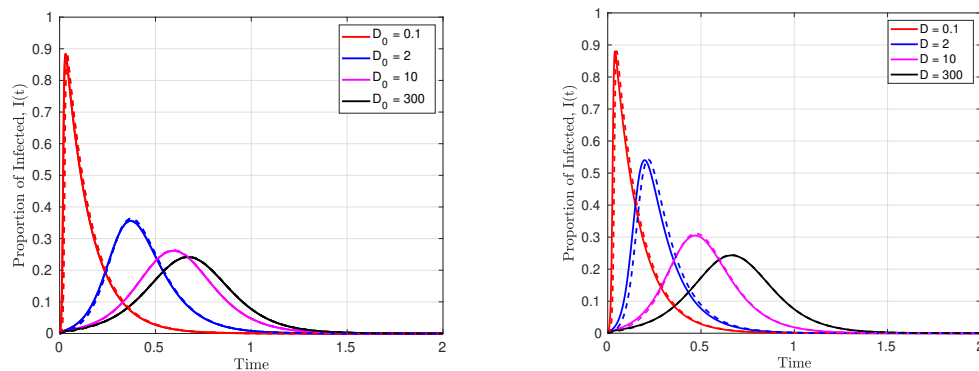
Similar to the results for a single population patch, epidemic take-off is delayed, and epidemic size decreases as the diffusion rate increases. When the diffusion rate is small, there is a delay in the epidemic take-off time in patch 2, and this delay decreases as the diffusion rate increases. The observed delays are due to the time it takes the pathogens shed in patch 1 to diffuse to patch 2, since there are no pathogens in the air, and no infections in patch 2 at the beginning of the epidemic. As the diffusion rate increases, the time it takes the pathogens to diffuse from patch 1 to patch 2 decreases, thereby decreasing the delay in epidemic take-off in the second population. In the limit where the diffusion rate becomes asymptotically large, the epidemics starts at approximately the same time in the two population patches for both models. Observe that the delay in epidemic take-off time in the second population is more obvious in the results from the coupled PDE-ODE model in Figure 4(b) than those of the reduced system of ODEs in Figure 4(a). This is because the system of ODEs is valid in the limit where the diffusion rate of the pathogens $D = \mathcal{O}(\nu^{-1})$, where $\nu = -1/\log \varepsilon$ with $\varepsilon \ll 1$. In this limit, the pathogens are already diffusing fast enough to reduce the time it takes them to travel from patch 1 to patch 2. This reduces the delay in take-off time of the epidemic in patch 2. As $D, D_0 \rightarrow \infty$, the system becomes well-mixed, and the predictions for the two model agree ($D = D_0 = 300$).

When there is a pathogen at the beginning of the outbreak ($P(0) = p(0) = 1$), with only one infected individual in patch 1 ($I_1(0) = 1/250$) and no infectives in patch 2 ($I_2(0) = 0$), the epidemics start



(a) Simulation of the reduced system of ODE (4.2). (b) Simulation of the coupled PDE-ODE (4.1).

Figure 4. The dynamics of the proportion of infected individuals $I(t)$ for different diffusion rates, and all other parameters as in Table 1. (a) shows the results for patches 1 and 2 obtained from the reduced system of ODEs (4.2) with initial conditions $(S_1(0), I_1(0), R_1(0)) = (249/250, 1/250, 0)$, $(S_2(0), I_2(0), R_2(0)) = (250/250, 0, 0)$ and $p(0) = 0$, and (b) shows similar results obtained with the coupled PDE-ODE model (4.1) for the same initial conditions in the patches as the ODEs and $P(0) = 0$ for the diffusing pathogens. In both plots, the solid lines represents patch 1, while the dashed lines are for patch 2.



(a) Simulation of the reduced system of ODE (4.2). (b) Simulation of the coupled PDE-ODE (4.1).

Figure 5. The dynamics of infected $I(t)$ for different diffusion rates of pathogen, and all other parameters as in Table 1. (a) shows the results obtained for patches 1 and 2 from the reduced system of ODEs (4.2) with initial conditions $(S_1(0), I_1(0), R_1(0)) = (249/250, 1/300, 0)$, $(S_2(0), I_2(0), R_2(0)) = (250/250, 0, 0)$, and $p(0) = 1$, while (b) shows similar results obtained from the coupled PDE-ODE model (4.1) with the same initial conditions for the ODEs in the patches and $P(0) = 1$ for the diffusing pathogens. In both plots, the solid lines represent of patch 1, while the dashed lines are for patch 2.

in the two patches at approximately the same time for both models, irrespective of the diffusion rate of pathogens. This occurs simply because there are pathogens in the air close to the second patch at time $t = 0$, which cause infections to spread into the population immediately. These results are shown in Figure 5. The parameters and initial conditions used are the same as those used for the results in Figure 4 except for the initial density of pathogen $p(0) = P(0) = 1$.

For a scenario with two distinct patches where the transmission of infections and shedding of pathogens are done at different rates (a more realistic scenario), the reduced system of ODEs (4.2) predicts slightly different results from the coupled PDE-ODE model (4.1). These results are shown in Figure 6. The dimensional transmission and shedding rates in patch 1 are $\mu_1 = 0.3$ and $r_1 = 0.1$, respectively, while in patch 2 are $\mu_2 = 1.2$ and $r_2 = 1$ respectively (their dimensionless equivalents can be computed with (2.8)). Figures 6(a) and 6(b) show the proportion of infected individuals in patches 1 and 2, respectively, obtained using the reduced system of ODEs (4.2) with different values of D_0 , while Figures 6(c) and 6(d) show similar results for the coupled PDE-ODE model (4.1). We observe from these figures that even though there are no infections in patch 2 when the outbreak begins, there are still more infections occurring in patch 2 than in patch 1. This occurs simply because patch 2 has a higher shedding and transmission rate. Higher shedding and transmission rates imply more pathogens are shed and transmitted faster in patch 2 than in patch 1.

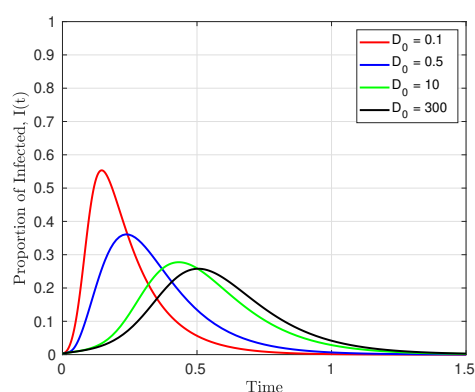
When the diffusion rate is small or asymptotically large, the estimates from the two models agree qualitatively. However, this is not the case for intermediate diffusion rates. For these rates, the coupled PDE-ODE model shows no significant difference in the epidemic take-off times in patch 1 for different values of D , although, the maximum number of proportion of infectives at a given time is different (see the results for $D = 0.5$ and $D = 10$ in Figure 6(c)). This is due to the fact that the transmission and shedding of pathogens are done at higher rates in patch 2 relative to patch 1. The pathogens shed in patch 2 diffuse to patch 1, thereby causing the epidemic in patch 1 to occur earlier than one would have expected if the populations were identical or the patches are farther away from each other. As the distance between the two patches increases, the effect of the pathogens shed in patch 2 on the population in patch 1 decreases. This qualitative effect is discussed in detail in Section 5, where we study the effect of patch locations on the spread of infections.

5. Effect of patch location on the spread of infection

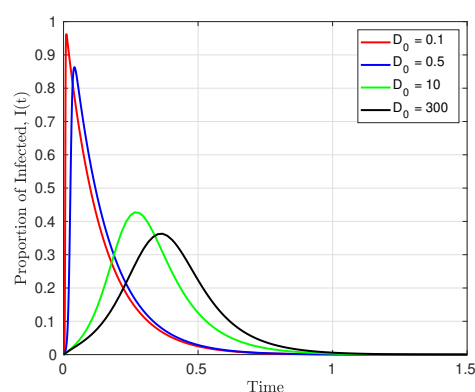
So far, we have studied the effect of the diffusion rate of pathogens on the spread of infections within and between populations, and we have not considered the effect of the location of the patches. In this section, we study the effect of patch location on the dynamics of infections by analyzing the two-term (extended model) reduced system of ODEs, as given in (2.31), which involves the Neumann Green's matrix characterizing the spatial interaction between patches. This extended ODE system is then used to compute the basic reproduction number and the final size relation, which now depends on the locations of the patches. In addition, we present some numerical simulations for two patches equally-placed on a ring of radius r , with $0 < r < 1$, concentric within a unit disk, and we study how the proportion of infected individuals changes as the distance between the patch locations is varied.

5.1. Effect of patch location on the basic reproduction number

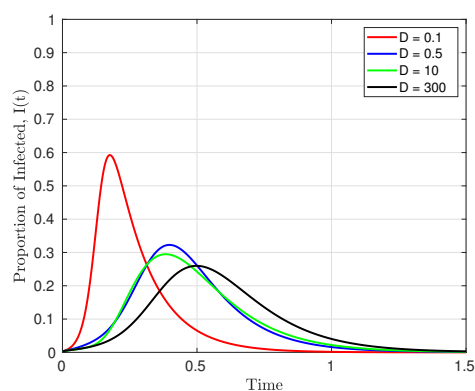
In our analysis below we assume that our domain is a unit disk and that the patches are equally-



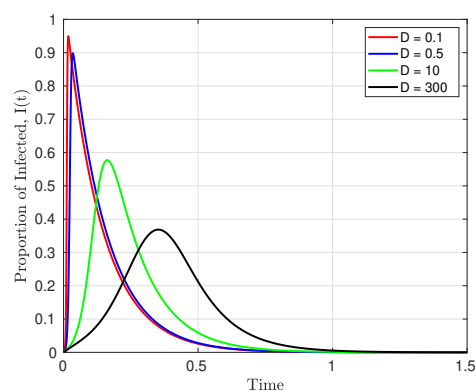
(a) Patch 1 for ODE model (4.2).



(b) Patch 2 for ODE model (4.2).



(c) Patch 1 for coupled PDE-ODE model (4.1).



(d) Patch 2 for coupled PDE-ODE model (4.1).

Figure 6. The dynamics of infected $I(t)$ for different diffusion rates, and all other parameters as in Table 2. (a) and (b) show the results obtained from the reduced system of ODEs (4.2) for patches 1 and 2, respectively, with initial conditions $(S_1(0), I_1(0), R_1(0)) = (299/300, 1/300, 0)$, $(S_2(0), I_2(0), R_2(0)) = (250/250, 0, 0)$, and $p(0) = 1$, while (c) and (d) show similar results obtained by solving the coupled PDE-ODE model (4.1) with the same initial conditions for the ODEs in the patches, and with $P(0) = 1$ for the diffusing pathogens.

placed on a ring of radius r , with $0 < r < 1$, which is concentric within the disk. Here, we derive an expression for the basic reproduction number using (2.31), while following the analytical framework used in Section 4. From the reduced system of ODEs (2.31), we construct our infectious classes for m patches as

$$\begin{aligned} \frac{dI_j}{dt} &= \beta_j S_j \left(P_0(t) + \frac{\sigma_j I_j}{2\pi D_0} \right) + \frac{\nu}{D_0} \beta_j S_j \Psi_j - \phi_j I_j, \quad j = 1, \dots, m, \\ \frac{dp}{dt} &= -p + \frac{1}{|\Omega|} \sum_{j=1}^m \sigma_j I_j. \end{aligned} \tag{5.1}$$

Here, $\Psi_j = (\mathcal{G}\Phi)_j$ is the j^{th} entry of the vector $\mathcal{G}\Phi$, with $\Phi = (\sigma_1 I_1, \dots, \sigma_m I_m)^T$, and \mathcal{G} is the Neumann Green's matrix defined in (2.32). The resulting ODE system is an $(m + 1)$ dimensional system of equations for the infected classes I_1, \dots, I_m , and the pathogens p . At the disease free equilibrium state, we construct the Jacobian matrix F for the new infections as

$$F = \left(\frac{\partial \mathcal{F}_i}{\partial x_j} \right)_{i,j} = \begin{pmatrix} \frac{\beta_1 N_1(0)}{D_0} \left(\frac{\sigma_1}{2\pi} + \nu \frac{\partial \Psi_1}{\partial I_1} \right) & \frac{\nu \beta_2 N_2(0)}{D_0} \frac{\partial \Psi_1}{\partial I_2} & \dots & \frac{\nu \beta_m N_m(0)}{D_0} \frac{\partial \Psi_1}{\partial I_m} & \beta_1 N_1(0) \\ \frac{\nu \beta_1 N_1(0)}{D_0} \frac{\partial \Psi_2}{\partial I_1} & \frac{\beta_2 N_2(0)}{D_0} \left(\frac{\sigma_2}{2\pi} + \nu \frac{\partial \Psi_2}{\partial I_2} \right) & \dots & \frac{\nu \beta_m N_m(0)}{D_0} \frac{\partial \Psi_2}{\partial I_m} & \beta_2 N_2(0) \\ \vdots & \vdots & \ddots & \vdots & \vdots \\ \frac{\nu \beta_1 N_1(0)}{D_0} \frac{\partial \Psi_m}{\partial I_1} & \frac{\nu \beta_2 N_2(0)}{D_0} \frac{\partial \Psi_m}{\partial I_2} & \dots & \frac{\beta_m N_m(0)}{D_0} \left(\frac{\sigma_m}{2\pi} + \nu \frac{\partial \Psi_m}{\partial I_m} \right) & \beta_m N_m^0 \\ 0 & 0 & 0 & 0 & 0 \end{pmatrix}, \tag{5.2}$$

where the functions $\mathcal{F}_j \equiv I_j'$ for $j = 1, \dots, m$, and $\mathcal{F}_{m+1} \equiv p'$ are as given in (5.1), $x_j \equiv I_j$ for $j = 1, \dots, m$, and $x_{m+1} \equiv p$. Similarly, from (5.1), we construct the Jacobian matrix V for the transfer of infections between compartments, evaluated at the disease free equilibrium state as

$$V = \left(\frac{\partial \mathcal{V}_i}{\partial x_j} \right)_{i,j} = \begin{pmatrix} \phi_1 & 0 & 0 & \dots & 0 \\ 0 & \phi_2 & 0 & \dots & 0 \\ \vdots & \vdots & \ddots & \vdots & 0 \\ 0 & 0 & 0 & \dots & \phi_m \\ -\frac{\sigma_1}{|\Omega|} & -\frac{\sigma_2}{|\Omega|} & \dots & -\frac{\sigma_m}{|\Omega|} & 1 \end{pmatrix}. \tag{5.3}$$

For the case of two population patches, the Jacobian matrices (5.2) and (5.3) reduce to

$$F = \begin{pmatrix} \frac{\beta_1 N_1(0)}{D_0} \left(\frac{\sigma_1}{2\pi} + \nu \frac{\partial \Psi_1}{\partial I_1} \right) & \frac{\nu \beta_2 N_2(0)}{D_0} \frac{\partial \Psi_1}{\partial I_2} & \beta_1 N_1(0) \\ \frac{\nu \beta_1 N_1(0)}{D_0} \frac{\partial \Psi_2}{\partial I_1} & \frac{\beta_2 N_2(0)}{D_0} \left(\frac{\sigma_2}{2\pi} + \nu \frac{\partial \Psi_2}{\partial I_2} \right) & \beta_2 N_2(0) \\ 0 & 0 & 0 \end{pmatrix} \quad \text{and} \quad V = \begin{pmatrix} \phi_1 & 0 & 0 \\ 0 & \phi_2 & 0 \\ -\frac{\sigma_1}{|\Omega|} & -\frac{\sigma_2}{|\Omega|} & 1 \end{pmatrix}.$$

Upon calculating the inverse of the matrix V , and then multiplying by the matrix F from the left, we construct our next generational matrix as

$$FV^{-1} = \begin{pmatrix} \frac{\beta_1 N_1(0)}{\phi_1 D_0} \left(\frac{\sigma_1}{2\pi} + \frac{\sigma_1 D_0}{|\Omega|} + \nu \frac{\partial \Psi_1}{\partial I_1} \right) & \frac{\nu \beta_2 N_2(0)}{\phi_2 D_0} \frac{\partial \Psi_1}{\partial I_2} + \frac{\sigma_2 \beta_1 N_1(0)}{\phi_2 |\Omega|} & \beta_1 N_1(0) \\ \frac{\nu \beta_1 N_1(0)}{\phi_1 D_0} \frac{\partial \Psi_2}{\partial I_1} + \frac{\sigma_1 \beta_2 N_2(0)}{\phi_1 |\Omega|} & \frac{\beta_2 N_2(0)}{\phi_2 D_0} \left(\frac{\sigma_2}{2\pi} + \frac{\sigma_2 D_0}{|\Omega|} + \nu \frac{\partial \Psi_2}{\partial I_2} \right) & \beta_2 N_2(0) \\ 0 & 0 & 0 \end{pmatrix}. \quad (5.4)$$

The dominant eigenvalue of the next generational matrix is our desired basic reproduction number. From a computation of the eigenvalues of (5.4), we derive a two term asymptotic expansion for the basic reproduction number given by

$$\mathcal{R} = \mathcal{R}^0 + \nu \mathcal{R}^1 + O(\nu^2), \quad (5.5)$$

where $\mathcal{R}^0 \equiv \mathcal{R}_0$ is the leading-order basic reproduction number given in (4.8), and the $O(\nu)$ term \mathcal{R}^1 is given by

$$\mathcal{R}^1 = \frac{1}{\phi_1 \phi_2 D_0} \left[\frac{\blacktriangle}{2} + \frac{4\pi \phi_1 \phi_2 D_0 \blacktriangle \blacksquare + (|\Omega| + 2\pi D_0) \blacktriangledown \spadesuit}{\sqrt{(|\Omega|^2 + 4\pi |\Omega| D_0) \spadesuit^2 + 4\pi^2 D_0^2 \clubsuit^2}} \right], \quad (5.6)$$

where the quantities \blacktriangle , \blacktriangledown and \blacktriangleleft , are defined by

$$\begin{aligned} \blacktriangle &\equiv \beta_1 N_1(0) \phi_2 \frac{\partial \Psi_1}{\partial I_1} + \beta_2 N_2(0) \phi_1 \frac{\partial \Psi_2}{\partial I_2}, & \blacktriangledown &\equiv \beta_1 N_1(0) \phi_2 \frac{\partial \Psi_1}{\partial I_1} - \beta_2 N_2(0) \phi_1 \frac{\partial \Psi_2}{\partial I_2}, \\ \blacktriangleleft &\equiv (\beta_1 N_1(0))^2 \sigma_2 \frac{\partial \Psi_2}{\partial I_1} + (\beta_2 N_2(0))^2 \sigma_1 \frac{\partial \Psi_1}{\partial I_2}. \end{aligned} \quad (5.7)$$

Here, the variables \spadesuit and \clubsuit are as defined in (4.8), and Ψ_j for $j = 1, 2$ are as defined in (2.31). Since there are only two patches, we can use (2.31) to construct Ψ_1 and Ψ_2 explicitly as

$$\Psi_1 = \sigma_1 I_1 \mathfrak{R}_1 + \sigma_2 I_2 G(\mathbf{x}_1; \mathbf{x}_2), \quad \text{and} \quad \Psi_2 = \sigma_1 I_1 G(\mathbf{x}_2; \mathbf{x}_1) + \sigma_2 I_2 \mathfrak{R}_2,$$

where $\mathfrak{R}_j \equiv \mathfrak{R}(\mathbf{x}_j)$ is the regular part of the Neumann Green's function $G(\mathbf{x}_i; \mathbf{x}_j)$ at $\mathbf{x} = \mathbf{x}_j$. Upon differentiating Ψ_1 and Ψ_2 , with respect to I_1 and I_2 , we obtain

$$\frac{\partial \Psi_1}{\partial I_1} = \sigma_1 \mathfrak{R}_1, \quad \frac{\partial \Psi_1}{\partial I_2} = \sigma_2 G(\mathbf{x}_1; \mathbf{x}_2), \quad \frac{\partial \Psi_2}{\partial I_1} = \sigma_1 G(\mathbf{x}_2; \mathbf{x}_1), \quad \text{and} \quad \frac{\partial \Psi_2}{\partial I_2} = \sigma_2 \mathfrak{R}_2. \quad (5.8)$$

To evaluate these derivatives explicitly, as are needed in (5.7), we must determine the Neumann Green's function $G(\mathbf{x}_i; \mathbf{x}_j)$ and its regular part \mathfrak{R}_j , as obtained by solving (2.25) in the unit disk. These results are well-known (see equation (4.3) of [20]), and we have

$$\begin{aligned} G(\mathbf{x}; \boldsymbol{\xi}) &= -\frac{1}{2\pi} \log |\mathbf{x} - \boldsymbol{\xi}| - \frac{1}{4\pi} \log \left(|\mathbf{x}|^2 |\boldsymbol{\xi}|^2 + 1 - 2\mathbf{x} \cdot \boldsymbol{\xi} \right) + \frac{(|\mathbf{x}|^2 + |\boldsymbol{\xi}|^2)}{4\pi} - \frac{3}{8\pi}, \\ \mathfrak{R}(\boldsymbol{\xi}) &= -\frac{1}{2\pi} \log (1 - |\boldsymbol{\xi}|^2) + \frac{|\boldsymbol{\xi}|^2}{2\pi} - \frac{3}{8\pi}. \end{aligned} \quad (5.9)$$

Since the patches are symmetrically located on a ring of radius r , with $0 < r < 1$, we can take their centers as $\mathbf{x}_1 = (r, 0)$ and $\mathbf{x}_2 = (-r, 0)$ for patch 1 and 2, respectively, so that, $|\mathbf{x}_1| = |\mathbf{x}_2| = r$. Substituting \mathbf{x}_1 and \mathbf{x}_2 into (5.9), we conclude that

$$\begin{aligned} G(\mathbf{x}_1; \mathbf{x}_2) = G(\mathbf{x}_2; \mathbf{x}_1) &= \frac{1}{2\pi} \left(-\log(2r) - \log(1 + r^2) + r^2 - \frac{3}{4} \right), \\ \Re(\mathbf{x}_1) = \Re(\mathbf{x}_2) &= \frac{1}{2\pi} \left(-\log(1 - r^2) + r^2 - \frac{3}{4} \right). \end{aligned} \quad (5.10)$$

Upon substituting (5.10) into (5.8), and then using (5.8) in (5.7), we obtain

$$\begin{aligned} \blacktriangle &\equiv \frac{\clubsuit}{2\pi} \left(-\log(1 - r^2) + r^2 - \frac{3}{4} \right), & \blacktriangledown &\equiv \frac{\spadesuit}{2\pi} \left(-\log(1 - r^2) + r^2 - \frac{3}{4} \right), \\ \blacksquare &\equiv \frac{\sigma_1 \sigma_2}{2\pi} \left(-\log(2r) - \log(1 + r^2) + r^2 - \frac{3}{4} \right) \left[(\beta_1 N_1(0))^2 + (\beta_2 N_2(0))^2 \right], \end{aligned} \quad (5.11)$$

where \clubsuit and \spadesuit are given by

$$\clubsuit = \beta_1 N_1(0) \phi_2 \sigma_1 + \beta_2 N_2(0) \phi_1 \sigma_2 \quad \text{and} \quad \spadesuit = \beta_1 N_1(0) \phi_2 \sigma_1 - \beta_2 N_2(0) \phi_1 \sigma_2. \quad (5.12)$$

Therefore, the $O(\nu)$ term in the basic reproduction number (5.5) can be computed by substituting (5.12) and (5.11) into (5.6). By using the leading-order basic reproduction number \mathcal{R}^0 , as given in (4.8), together with \mathcal{R}^1 in (5.5), we arrive at an explicit two term asymptotic expansion for the basic reproduction \mathcal{R} , which depends on the locations of the patches. Notice that the dependence on the location comes into \mathcal{R} through only the $O(\nu)$ term, which involves the Green's function.

5.2. Effect of patch location on the final size relation

In the previous subsection, for a special two-patch configuration where the patches are equally spaced on a ring concentric within the disk, we derived a two-term asymptotic formula for the basic reproduction number. In this subsection, we study the effect of patch location on the final size of the epidemic.

From (2.31), a two term asymptotic expansion of the reduced system of ODEs for the case of two population patches is given by

$$\frac{dp}{dt} = -p + \frac{1}{|\Omega|} (\sigma_1 I_1 + \sigma_2 I_2), \quad (5.13a)$$

Patch 1

$$\frac{dS_1}{dt} = -\beta_1 S_1 p - \beta_1 S_1 \left(\frac{\sigma_1 I_1}{2\pi D_0} \right) - \frac{\nu}{D_0} \beta_1 S_1 \Psi_1$$

$$\frac{dI_1}{dt} = \beta_1 S_1 p + \beta_1 S_1 \left(\frac{\sigma_1 I_1}{2\pi D_0} \right) + \frac{\nu}{D_0} \beta_1 S_1 \Psi_1 - \phi_1 I_1,$$

$$\frac{dR_1}{dt} = \phi_1 I_1,$$

Patch 2

$$\frac{dS_2}{dt} = -\beta_2 S_2 p - \beta_2 S_2 \left(\frac{\sigma_2 I_2}{2\pi D_0} \right) - \frac{\nu}{D_0} \beta_2 S_2 \Psi_2,$$

$$\frac{dI_2}{dt} = \beta_2 S_2 p + \beta_2 S_2 \left(\frac{\sigma_2 I_2}{2\pi D_0} \right) + \frac{\nu}{D_0} \beta_2 S_2 \Psi_2 - \phi_2 I_2,$$

$$(5.13b)$$

$$\frac{dR_2}{dt} = \phi_2 I_2,$$

where $p(t)$ is the leading-order density of pathogens in the air, S_j, I_j, R_j are the susceptible, infected, and removed, respectively, in the j^{th} patch for $j = 1, 2$. Here, $\Psi_1 = \sigma_1 I_1 \mathfrak{R}_1 + \sigma_2 I_2 G(\mathbf{x}_1; \mathbf{x}_2)$ and $\Psi_2 = \sigma_1 I_1 G(\mathbf{x}_2; \mathbf{x}_1) + \sigma_2 I_2 \mathfrak{R}_2$, and $G(\mathbf{x}_1; \mathbf{x}_2) = G(\mathbf{x}_1; \mathbf{x}_1)$ is the Neumann Green's function and $\mathfrak{R}_1 = \mathfrak{R}_2$ is its regular part at the points \mathbf{x}_1 and \mathbf{x}_2 . This system of ODEs depends on the locations of the patches, and the dependence arises from the $O(\nu)$ terms.

Following the same approach as in subsection (4.2), we integrate the S_1 and S_2 equations in (5.13b) to obtain

$$\log \frac{S_{10}}{S_{1\infty}} = \beta_1 \int_0^\infty p(t) dt + \frac{\beta_1 \sigma_1}{2\pi D_0} \int_0^\infty I_1(t) dt + \frac{\beta_1 \nu}{D_0} \int_0^\infty \Psi_1 dt. \quad (5.14)$$

and

$$\log \frac{S_{20}}{S_{2\infty}} = \beta_2 \int_0^\infty p(t) dt + \frac{\beta_2 \sigma_2}{2\pi D_0} \int_0^\infty I_2(t) dt + \frac{\beta_2 \nu}{D_0} \int_0^\infty \Psi_2 dt. \quad (5.15)$$

The integrals of Ψ_1 and Ψ_2 are given by

$$\int_0^\infty \Psi_1 dt = \sigma_1 \mathfrak{R}_1 \int_0^\infty I_1(t) dt + \sigma_2 G(\mathbf{x}_1; \mathbf{x}_2) \int_0^\infty I_2(t) dt$$

and

$$\int_0^\infty \Psi_2 dt = \sigma_1 G(\mathbf{x}_2; \mathbf{x}_1) \int_0^\infty I_1(t) dt + \sigma_2 \mathfrak{R}_2 \int_0^\infty I_2(t) dt$$

Similarly, the integral of (5.13a) is given by (4.14). Upon substituting (4.14) into (5.14) and (5.15), and assuming that the outbreak begins with no epidemic ($p_0 = 0$), the final size relation is given by

$$\begin{aligned} \log \frac{S_{10}}{S_{1\infty}} &= \frac{\beta_1 \sigma_1 N_1(0)}{\phi_1 |\Omega|} \left\{ 1 - \frac{S_{1\infty}}{N_1(0)} \right\} + \frac{\beta_1 \sigma_2 N_2(0)}{\phi_2 |\Omega|} \left\{ 1 - \frac{S_{2\infty}}{N_2(0)} \right\} + \frac{\beta_1 \sigma_1 N_1(0)}{2\pi \phi_1 D_0} \left\{ 1 - \frac{S_{1\infty}}{N_1(0)} \right\} \\ &\quad + \frac{\beta_1 \nu}{D_0} \left[\frac{\sigma_1 \mathfrak{R}_1 N_1(0)}{\phi_1} \left\{ 1 - \frac{S_{1\infty}}{N_1(0)} \right\} + \frac{\sigma_2 G(\mathbf{x}_1; \mathbf{x}_2) N_2(0)}{\phi_2} \left\{ 1 - \frac{S_{2\infty}}{N_2(0)} \right\} \right], \end{aligned}$$

and

$$\begin{aligned} \log \frac{S_{20}}{S_{2\infty}} &= \frac{\beta_2 \sigma_1 N_1(0)}{\phi_1 |\Omega|} \left\{ 1 - \frac{S_{1\infty}}{N_1(0)} \right\} + \frac{\beta_2 \sigma_2 N_2(0)}{\phi_2 |\Omega|} \left\{ 1 - \frac{S_{2\infty}}{N_2(0)} \right\} + \frac{\beta_2 \sigma_2 N_2(0)}{2\pi \phi_2 D_0} \left\{ 1 - \frac{S_{2\infty}}{N_2(0)} \right\} \\ &\quad + \frac{\beta_2 \nu}{D_0} \left[\frac{\sigma_2 \mathfrak{R}_2 N_2(0)}{\phi_2} \left\{ 1 - \frac{S_{2\infty}}{N_2(0)} \right\} + \frac{\sigma_1 G(\mathbf{x}_2; \mathbf{x}_1) N_1(0)}{\phi_1} \left\{ 1 - \frac{S_{1\infty}}{N_1(0)} \right\} \right], \end{aligned}$$

which can be written as

$$\begin{aligned} \log \frac{S_{10}}{S_{1\infty}} &= \beta_1 \left(\mathfrak{R}_1 \left\{ 1 - \frac{S_{1\infty}}{N_1(0)} \right\} + \mathfrak{R}_2 \left\{ 1 - \frac{S_{2\infty}}{N_2(0)} \right\} + \frac{\sigma_1 N_1(0)}{2\pi \phi_1 D_0} \left\{ 1 - \frac{S_{1\infty}}{N_1(0)} \right\} \right. \\ &\quad \left. + \frac{\nu}{D_0} \left[\frac{\sigma_1 \mathfrak{R}_1 N_1(0)}{\phi_1} \left\{ 1 - \frac{S_{1\infty}}{N_1(0)} \right\} + \frac{\sigma_2 G(\mathbf{x}_1; \mathbf{x}_2) N_2(0)}{\phi_2} \left\{ 1 - \frac{S_{2\infty}}{N_2(0)} \right\} \right] \right), \quad (5.16) \\ \log \frac{S_{20}}{S_{2\infty}} &= \beta_2 \left(\mathfrak{R}_1 \left\{ 1 - \frac{S_{1\infty}}{N_1(0)} \right\} + \mathfrak{R}_2 \left\{ 1 - \frac{S_{2\infty}}{N_2(0)} \right\} + \frac{\sigma_2 N_2(0)}{2\pi \phi_2 D_0} \left\{ 1 - \frac{S_{2\infty}}{N_2(0)} \right\} \right. \\ &\quad \left. + \frac{\nu}{D_0} \left[\frac{\sigma_2 \mathfrak{R}_2 N_2(0)}{\phi_2} \left\{ 1 - \frac{S_{2\infty}}{N_2(0)} \right\} + \frac{\sigma_1 G(\mathbf{x}_2; \mathbf{x}_1) N_1(0)}{\phi_1} \left\{ 1 - \frac{S_{1\infty}}{N_1(0)} \right\} \right] \right), \end{aligned}$$

where $\mathcal{R}_1 = \sigma_1 N_1(0)/(\phi_1 |\Omega|)$ and $\mathcal{R}_2 = \sigma_2 N_2(0)/(\phi_2 |\Omega|)$. Upon writing (5.16) in matrix form, we have

$$\begin{pmatrix} \log \frac{S_{10}}{S_{1\infty}} \\ \log \frac{S_{20}}{S_{2\infty}} \end{pmatrix} = \left(\mathbb{A} + \mathbb{B} + \frac{\nu}{D_0} \mathbb{C} \right) \begin{pmatrix} 1 - \frac{S_{1\infty}}{N_1(0)} \\ 1 - \frac{S_{2\infty}}{N_2(0)} \end{pmatrix}, \quad (5.17)$$

where the matrices \mathbb{A} , \mathbb{B} , and \mathbb{C} are defined by

$$\mathbb{A} = \begin{pmatrix} \beta_1 \mathcal{R}_1 & \beta_1 \mathcal{R}_2 \\ \beta_2 \mathcal{R}_1 & \beta_2 \mathcal{R}_2 \end{pmatrix}, \quad \mathbb{B} = \begin{pmatrix} \frac{\sigma_1 \beta_1 N_1(0)}{2\pi \phi_1 D_0} \\ \frac{\sigma_2 \beta_2 N_2(0)}{2\pi \phi_2 D_0} \end{pmatrix} \quad \text{and} \quad \mathbb{C} = \begin{pmatrix} \frac{\sigma_1 \beta_1 \mathfrak{R}_1 N_1(0)}{\phi_1} & \frac{\sigma_2 \beta_1 G(\mathbf{x}_1; \mathbf{x}_2) N_2(0)}{\phi_2} \\ \frac{\sigma_1 \beta_2 G(\mathbf{x}_2; \mathbf{x}_1) N_1(0)}{\phi_1} & \frac{\sigma_2 \beta_2 \mathfrak{R}_2 N_2(0)}{\phi_2} \end{pmatrix}.$$

In this way, we have derived a two term expansion of the final size relation that depends on the location of the patches. Similar to the basic reproduction number (5.5), the dependence on the location comes into this result at the $\mathcal{O}(\nu)$ term through the Green's function and its regular part. The explanation of the final size follows from subsection 4.2.

5.3. Numerical simulation for two patch model with effect of patch location

Next, we present some surface plots of the basic reproduction number \mathcal{R} in (5.5) and its $\mathcal{O}(\nu)$ correction term \mathcal{R}^1 , defined in (5.6), with respect to the location of the patches. Our plots are for different values of the dimensionless transmission rates β_1 and β_2 for patches 1 and 2, respectively. In addition, we show some numerical simulations of the reduced system of ODEs (5.13) and the coupled PDE-ODE model (4.1) for two patches. The system of ODEs is solved using the MATLAB numerical ODE solver *ODE45* [25], while the PDE is solved using *FlexPDE* [26]. Our goal is to numerically study the effect of patch location on the spread of infections and the final epidemic size.

Figure 7 shows the surface plot of the $\mathcal{O}(\nu)$ term of the basic reproduction number, \mathcal{R}^1 (5.6) (first row), and the basic reproduction number \mathcal{R} (5.5) (second row) with respect to the location of the patches and the transmission rates of the two patches. For each of the results in this figure, the transmission rate β_1 (vertical axis) is plotted against the distance of the patches from the center of the unit disk (horizontal axis). A fixed value of β_2 is used for each column, with the value increasing from left to right ($\beta_2 = 0.1, 0.4, 0.8, 1.2$). Since r is the distance from the center of each patch to the center of the unit disk, for each value of r , the distance between the centers of the two patches is $2r$. The $\mathcal{O}(\nu)$ term \mathcal{R}^1 shows how the leading-order basic reproduction number $\mathcal{R}^0 \equiv \mathcal{R}_0$ (4.9) is perturbed by the locations of the patches. Note that we have omitted the surface plots of \mathcal{R}^0 from this figure because it is independent on the location of the patches.

The first row of Figure 7 shows that \mathcal{R}^1 may increase or decrease \mathcal{R} depending on the location of the patches and the transmission rates. When the transmission rate in patch 2 is $\beta_2 = 0.1$ (Figures 7(a)), we observe that \mathcal{R}^1 has high values when r is small and β_1 is high. In this case, where the two patches are close to each other, the infection is transmitted at a high rate in patch 1. As the distance between the

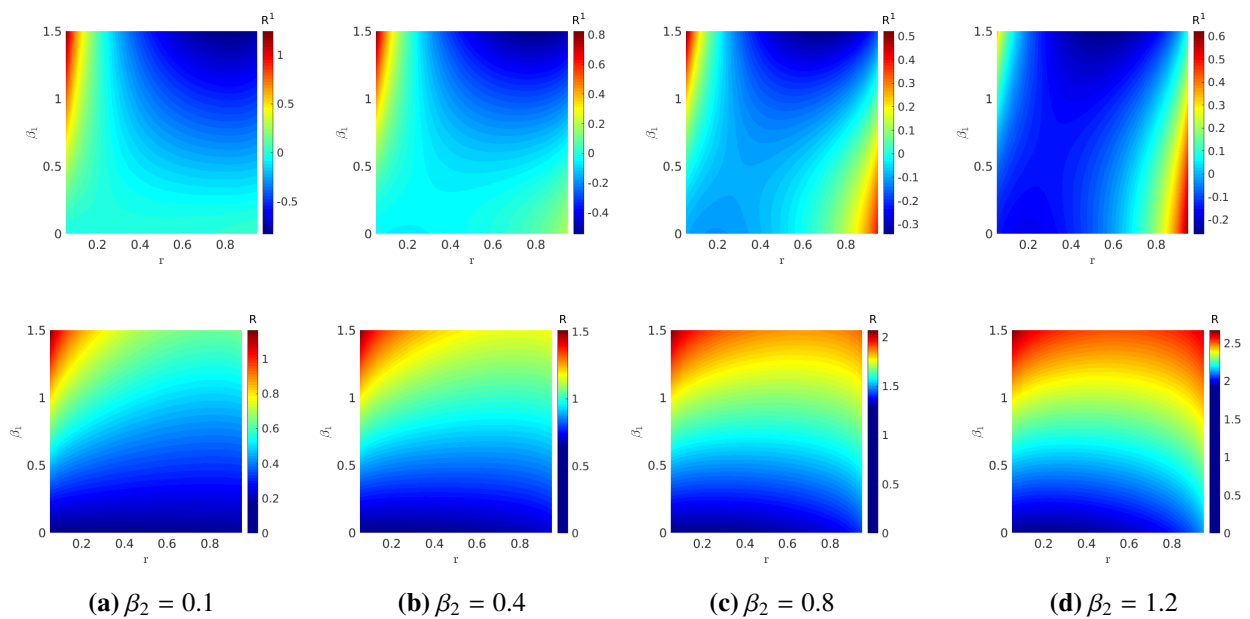


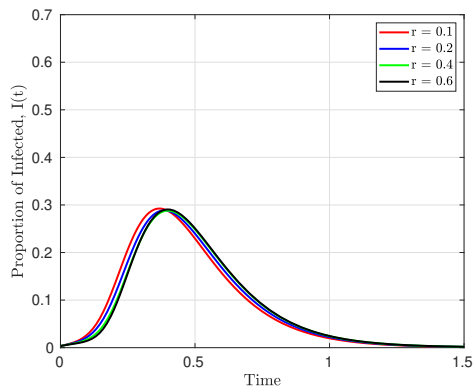
Figure 7. Surface plots of the basic reproduction number \mathcal{R} (5.5) (second row) and its $O(v)$ term \mathcal{R}^1 (5.6) (first row) with respect to the distance of the patches from the center of a unit disk r , for different values of the transmission rates β_1 and β_2 for patches 1 and 2, respectively. The parameters used are given in Table 2 except for $p_c = 450$, with diffusion rate $D_0 = 5$. For each of the graphs, β_1 (vertical axis) is plotted against r (horizontal axis). The value of β_2 changes for each column from left to right in increasing order. The term \mathcal{R}^1 shows how the leading-order basic reproduction number \mathcal{R}^0 is perturbed by the location of the patches.

two patches increases (r increases), the value of \mathcal{R}^1 decreases for all values of β_1 and it attains negative values for some values of β_1 . For this range, \mathcal{R}^1 decreases the leading-order basic reproduction number \mathcal{R}^0 . These figures show that for all values of β_2 , there are more infections (\mathcal{R} and \mathcal{R}^1 high) when the two patches are closer to each other (r small), as compared to when they are farther apart (r large). In addition, as the transmission rate β_2 increases (from left to right in Figure 7), the surface plot of \mathcal{R}^1 in the r, β_1 parameter space changes, and the effect of the reflecting boundary of the unit disk becomes apparent. For each value of β_2 , the corresponding effect of \mathcal{R}^1 on the overall basic reproduction number \mathcal{R} is shown in the second row of Figure 7. When $\beta_2 = 1.2$, we observe that higher values of \mathcal{R}^1 occur for smaller values of r (when the two patches are close to each other) and for values of r close to 1 (when the patches are close to the boundary of the disk). When the patches become closer to the reflecting boundary of the unit disk, they see a reflection of themselves through the boundary. This leads to a feedback-effect whereby the reflection of pathogen from the boundary returns back to the patches. This boundary effect, as evident in the surface plot of the basic reproduction number \mathcal{R} in Figure 7(d), leads to a higher level of infections.

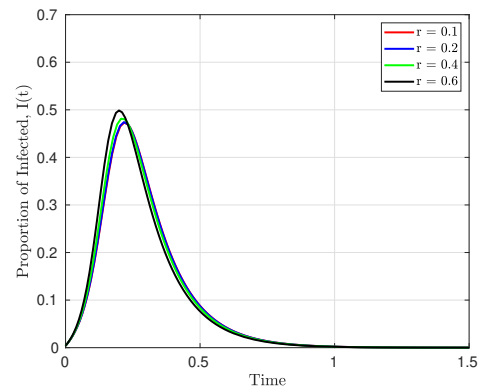
The numerical simulations of the coupled PDE-ODE model (4.1) and the reduced system of ODEs (5.13) for two patches in the unit disk are shown in Figure 8. For a fixed diffusion rate of pathogens, these two models are solved numerically for different locations of the patches. The location of each patch is given in terms of the parameter r , which measures the distance between the center of the patch and the center of the unit disk. Both patches have the same parameters except for the transmission rates of infection, and the shedding rate of pathogens (see Table 2). In addition, both patches have one infective at the beginning of the outbreak, and the density of pathogens in the air is fixed at $p(0) = P(0) = 1$.

Figures 8(a) and 8(b) show the results obtained from the reduced system of ODEs (5.13) for patches 1 and 2, respectively, while Figures 8(c) and 8(d) show similar results for the coupled PDE-ODE model (4.1). For each radius r , the epidemic in patch 2 (right column of Figure 8) is more than that in patch 1 for both models, owing to the fact that patch 2 has higher transmission and shedding rates than patch 1 (see Table 2 for the parameters). As the radius of the ring (on which the patches are located) increases, that is, as the distance between the centers of the two patches increases, the size of the epidemic in patch 1 decreases, while there seems to be no significant difference in the size of the epidemic in patch 2. Since the shedding rate of pathogens in patch 2 is larger than that of patch 1, the density of pathogens in the air around patch 2 at each point in time is higher than those around patch 1. As a result, when the two patches are closer to each other, the pathogens shed from patch 2 can easily diffuse to patch 1, and lead to more infections in the population. This effect depends on the proximity of the two patches, and it weakens as the patches move farther away from each other. This explains why infections in patch 1 decrease as the distance in the two patches increases. This observation is more prominent in the results obtained from the PDE-ODE model than in the the system of ODEs. This is due to the fact that the ODE system is valid in the limit $D \gg \mathcal{O}(\nu^{-1})$, with $\nu = -1/\log \varepsilon$ and $\varepsilon \ll 1$. In this regime where the pathogens are diffusing fast, spatial gradients in the pathogen density are smoothed out, and as a result the proximity of patch 2 to patch 1 seems to have no significant effect on the epidemic in patch 2.

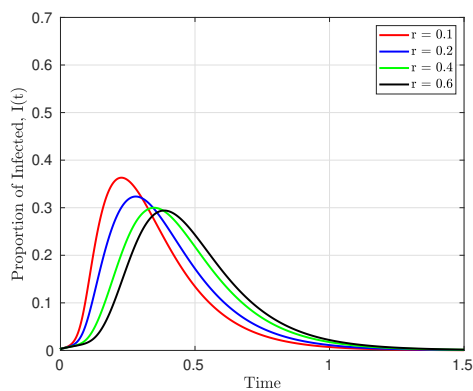
However, as both patches move closer to the boundary of the domain, they receive signals of pathogens that is of equal strength as their shedding rates from the boundary (since the boundary is reflecting). In this way, there is an increasing infection in both patches as they move closer to the boundary. This observation is noticeable in the patch 2 dynamics shown in Figures (8(b)) and (8(d)),



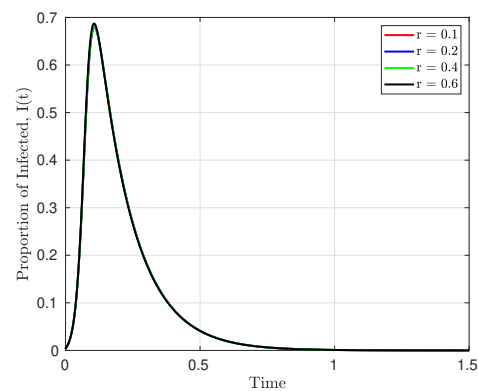
(a) Patch 1 for ODE model (4.2).



(b) Patch 2 for ODE model (4.2).



(c) Patch 1 for coupled PDE-ODE model (4.1).



(d) Patch 2 for coupled PDE-ODE model (4.1).

Figure 8. The dynamics of infected $I(t)$ for different ring radius r . (a) and (b) show the results obtained from the reduced system of ODEs (5.13) for patches 1 and 2, respectively, with initial conditions $(S_1(0), I_1(0), R_1(0)) = (299/300, 1/300, 0)$, $(S_2(0), I_2(0), R_2(0)) = (250/250, 0, 0)$, and $p(0) = 1$, while (c) and (d) show similar results obtained from the coupled PDE-ODE model (4.1) with the same initial conditions for the ODEs in the patches and $P(0) = 1$ for the diffusing pathogens. The diffusion rate of pathogens is fixed at $D_0 = D = 5$, while all other parameters are as given Table 2.

due to its high shedding rate. Specifically, it is more apparent in Figure 8(b) than in Figure 8(d) because the system of ODEs used to obtain Figure 8(b) are only valid in the limit where the pathogens are diffusing very fast. We observe from these simulations that the estimates and predictions of both models qualitatively agree, even though the ODE model is only valid in the limit $D \gg O(\nu^{-1})$.

6. Discussion

We developed and analyzed a coupled PDE-ODE model for studying the spread of airborne diseases with indirect transmission. This model improves previously developed epidemic models for indirect transmission [7, 13] by incorporating the movement of pathogens, which is modeled with linear diffusion. Human populations are modeled as circular patches, that are small relative to the length scale of the domain, where each patch has an SIR dynamics for the population of susceptible, infected, and removed, respectively. The diffusion of pathogens is restricted to the region outside the patches, while human movement is not considered. In our model, a susceptible individual becomes infected only by coming in contact with the pathogens (*indirect transmission*), and the spread of infection within a patch depends on the density of pathogens around the patch. In the limit $D = O(\nu^{-1})$ with $\nu = -1/\log \varepsilon$ and $\varepsilon \ll 1$ (when the pathogens are diffusing fast), the coupled PDE-ODE model is reduced to a nonlinear system of ODEs. This system of ODEs was then analyzed and used to compute the basic reproduction number and the final size relation. Furthermore, the full PDE-ODE model and the reduced system of ODEs were solved numerically, and their results agreed qualitatively.

The numerical simulations for both the coupled model and the reduced system of ODEs predicted a decrease in the epidemic as the diffusion rate of pathogens increases, and the two models agreed in the limit $D, D_0 \rightarrow \infty$. When pathogens are diffusing slowly, it takes longer for them to diffuse away from the patches after shedding, and as a result, more infections occur. On the other hand, when the diffusion rate is high, pathogens diffuse away from the patches immediately after shedding, which thereby reduces infections. When there are two patches, where infection starts from only one of the patches with the other patch being disease free, and with no pathogens in the air, our models predict a delay in epidemic take-off time in the second population when pathogens diffuse slowly. This occurs as a result of the time required for pathogens to diffuse from the infected patch to the other patch. As the diffusion rate increases, the delay in epidemic take-off time decreases. The results of our model seem consistent with other previous results [12, 17, 19, 22, 23, 29], where human populations were modeled with a PDE approach. Furthermore, we studied the effect of patch location on the spread of infection. Our models predicted more infections when the two patches are close to each other, and less infections when the patches are farther apart.

In our model, we have assumed that the amount of pathogens in a patch can be accounted for by knowing the density of pathogens around the patch, and individuals do not move between patches. This assumption may not be true for all real-life scenarios as the amount of pathogens in a patch may be different from the density around the patch. Also, people may move between cities and towns. Our model can be extended to incorporate human mobility between patches. This can be achieved by allowing both humans and pathogens to diffuse in the bulk region, or by using the approach of meta population dynamics, in which individuals are transferred from one patch to another without modeling their movement explicitly, or by using Lagrangian method to keep track of individuals' place of residence at different time. In addition to this, we can allow for infections to be transmitted in the

bulk region when a susceptible individual comes in contact with the diffusing pathogens. This would lead to a reaction-diffusion type model in the bulk region. Furthermore, similar models (indirect and/or direct transmission model) can be developed for other diseases such as malaria, where the mosquitoes diffuse in the bulk region and human populations are modeled with patches. Mosquito reservoirs can also be incorporated into the modeling framework, where an ODE system is used to describe the mosquito life cycle from egg to adult.

Notwithstanding all of these limitations and assumptions, we believe that our proposed novel approach to modeling airborne diseases, where the movement of pathogens is explicitly modeled with linear diffusion, will significantly contribute to knowledge and may be seen as a better approach. Our analysis and full numerical computations suggest that disease dynamics can be adequately studied with our more tractable reduced ODE model, instead of the more intricate PDE-ODE coupled model. The presence of the parameter D_0 in the reduced ODE system makes it easier to study the effect of diffusion on disease transmission. Furthermore, the extended system of ODEs, which includes weak spatial effects through a Green's interaction matrix, allowed us to study the effect of patch location on disease dynamics. Including this spatial information encoded in the Green's matrix allows for characterizing the effect of the spatial distribution of patches on disease transmission between spatially segregated populations.

7. Acknowledgments

Fred Brauer and Michael Ward gratefully acknowledge the support from the NSERC Discovery Grant program under OGPIN 203901-99 and 81541, respectively.

8. Conflict of interest

All authors declare no conflict of interest in this paper.

References

1. Julien Arino, Fred Brauer, P Van Den Driessche, James Watmough, and Jianhong Wu. A final size relation for epidemic models. *Mathematical Biosciences and Engineering*, 4(2):159, 2007.
2. Clive B Beggs. The airborne transmission of infection in hospital buildings: Fact or fiction? *Indoor and Built Environment*, 12(1-2):9–18, 2003.
3. Derdei Bichara, Yun Kang, Carlos Castillo-Chavez, Richard Horan, and Charles Perrings. SIS and SIR epidemic models under virtual dispersal. *Bulletin of Mathematical Biology*, 77(11):2004–2034, 2015.
4. Fred Brauer. Age-of-infection and the final size relation. *Math. Biosci. Eng.*, 5(4):681–690, 2008.
5. Fred Brauer. Epidemic models with heterogeneous mixing and treatment. *Bulletin of Mathematical Biology*, 70(7):1869, 2008.
6. Fred Brauer. A final size relation for epidemic models of vector-transmitted diseases. *Infectious Disease Modelling*, 2(1):12–20, 2017.

7. Fred Brauer. A new epidemic model with indirect transmission. *Journal of Biological Dynamics*, 11(sup2):285–293, 2017.
8. Fred Brauer. The final size of a serious epidemic. *Bulletin of mathematical biology*, 81(3):869–877, 2019.
9. Fred Brauer and Carlos Castillo-Chavez. *Mathematical models for communicable diseases*, volume 84. SIAM, 2012.
10. Fred Brauer and Carlos Castillo-Chavez. *Mathematical Models in Population Biology and Epidemiology*, volume 40. Springer, 2001.
11. Fred Brauer, Carlos Castillo-Chavez, and Zhilan Feng. *Mathematical models in epidemiology*, 2018.
12. Settapat Chinviriyasit and Wirawan Chinviriyasit. Numerical modelling of an SIR epidemic model with diffusion. *Applied Mathematics and Computation*, 216(2):395–409, 2010.
13. Jummy Funke David. Epidemic models with heterogeneous mixing and indirect transmission. *Journal of Biological Dynamics*, 12(1):375–399, 2018.
14. Odo Diekmann, Johan Andre Peter Heesterbeek, and Johan AJ Metz. On the definition and the computation of the basic reproduction ratio R_0 in models for infectious diseases in heterogeneous populations. *Journal of Mathematical Biology*, 28(4):365–382, 1990.
15. Jing Ge, Kwang Ik Kim, Zhigui Lin, and Huaiping Zhu. A SIS reaction–diffusion–advection model in a low-risk and high-risk domain. *Journal of Differential Equations*, 259(10):5486–5509, 2015.
16. Jia Gou and Michael J. Ward. An asymptotic analysis of a 2-D model of dynamically active compartments coupled by bulk diffusion. *Journal of Nonlinear Science*, 26(4):979–1029, 2016.
17. Haomin Huang and Mingxin Wang. The reaction-diffusion system for an SIR epidemic model with a free boundary. *Discrete & Continuous Dynamical Systems-Series B*, 20(7), 2015.
18. Chacha M Issarow, Nicola Mulder, and Robin Wood. Modelling the risk of airborne infectious disease using exhaled air. *Journal of Theoretical Biology*, 372:100–106, 2015.
19. Kwang Ik Kim and Zhigui Lin. Asymptotic behavior of an SEI epidemic model with diffusion. *Mathematical and Computer Modelling*, 47(11-12):1314–1322, 2008.
20. T. Kolokolnikov, M. S Titcombe, and M. J. Ward. Optimizing the fundamental Neumann eigenvalue for the Laplacian in a domain with small traps. *Europ. J. Appl. Math.*, 16(2):161–200, 2005.
21. Ming Liu and Yihong Xiao. Modeling and analysis of epidemic diffusion with population migration. *Journal of Applied Mathematics*, 2013, 2013.
22. El Mehdi Lotfi, Mehdi Maziane, Khalid Hattaf, and Noura Yousfi. Partial differential equations of an epidemic model with spatial diffusion. *International Journal of Partial Differential Equations*, 2014, 2014.
23. Fabio A Milner and Ruijun Zhao. Analysis of an SIR model with directed spatial diffusion. *Mathematical Population Studies*, 15(3):160–181, 2008.
24. CJ Noakes, CB Beggs, PA Sleight, and KG Kerr. Modelling the transmission of airborne infections in enclosed spaces. *Epidemiology & Infection*, 134(5):1082–1091, 2006.

25. Lawrence F Shampine and Mark W Reichelt. The Matlab ODE suite. *SIAM Journal on Scientific Computing*, 18(1):1–22, 1997.
26. PDE solutions Inc. FlexPDE 6, 2019.
27. Pauline Van den Driessche and James Watmough. Reproduction numbers and sub-threshold endemic equilibria for compartmental models of disease transmission. *Mathematical Biosciences*, 180(1-2):29–48, 2002.
28. Michael J. Ward and Joseph B. Keller. Strong localized perturbations of eigenvalue problems. *SIAM J. App. Math.*, 53(3):770–798, 1993.
29. Zhi-ting Xu and Dan-xia Chen. An SIS epidemic model with diffusion. *Applied Mathematics-A Journal of Chinese Universities*, 32(2):127–146, 2017.
30. Liang Zhang, Zhi-Cheng Wang, and Yan Zhang. Dynamics of a reaction–diffusion waterborne pathogen model with direct and indirect transmission. *Computers & Mathematics with Applications*, 72(1):202–215, 2016.
31. Najat Ziyadi, Said Boulite, M Lhassan Hbid, and Suzanne Touzeau. Mathematical analysis of a PDE epidemiological model applied to scrapie transmission. *Communications on Pure and Applied Analysis*, 7(3):659, 2008.



AIMS Press

©2018 J. F. David, S. A. Iyaniwura, M. J. Ward and F. Brauer, licensee AIMS Press. This is an open access article distributed under the terms of the Creative Commons Attribution License (<http://creativecommons.org/licenses/by/4.0>)